



Identification of new alpha-synuclein fibrillogenesis inhibitor using in silico structure-based virtual screening

Mehdi Sahihi, Fatma Gaci, Isabelle Navizet

► To cite this version:

Mehdi Sahihi, Fatma Gaci, Isabelle Navizet. Identification of new alpha-synuclein fibrillogenesis inhibitor using in silico structure-based virtual screening. *Journal of Molecular Graphics and Modelling*, 2021, 108, pp.108010. 10.1016/j.jmgm.2021.108010 . hal-03705000

HAL Id: hal-03705000

<https://hal.science/hal-03705000>

Submitted on 26 Jun 2022

HAL is a multi-disciplinary open access archive for the deposit and dissemination of scientific research documents, whether they are published or not. The documents may come from teaching and research institutions in France or abroad, or from public or private research centers.

L'archive ouverte pluridisciplinaire **HAL**, est destinée au dépôt et à la diffusion de documents scientifiques de niveau recherche, publiés ou non, émanant des établissements d'enseignement et de recherche français ou étrangers, des laboratoires publics ou privés.

- 1
- 2
- 3
- 4
- 5
- 6
- 7
- 8
- 9
- 10
- 11
- 12
- 13
- 14
- 15
- 16
- 17
- 18
- 19

2

3

4

5

6

7

8

9

10

11

12

13

14

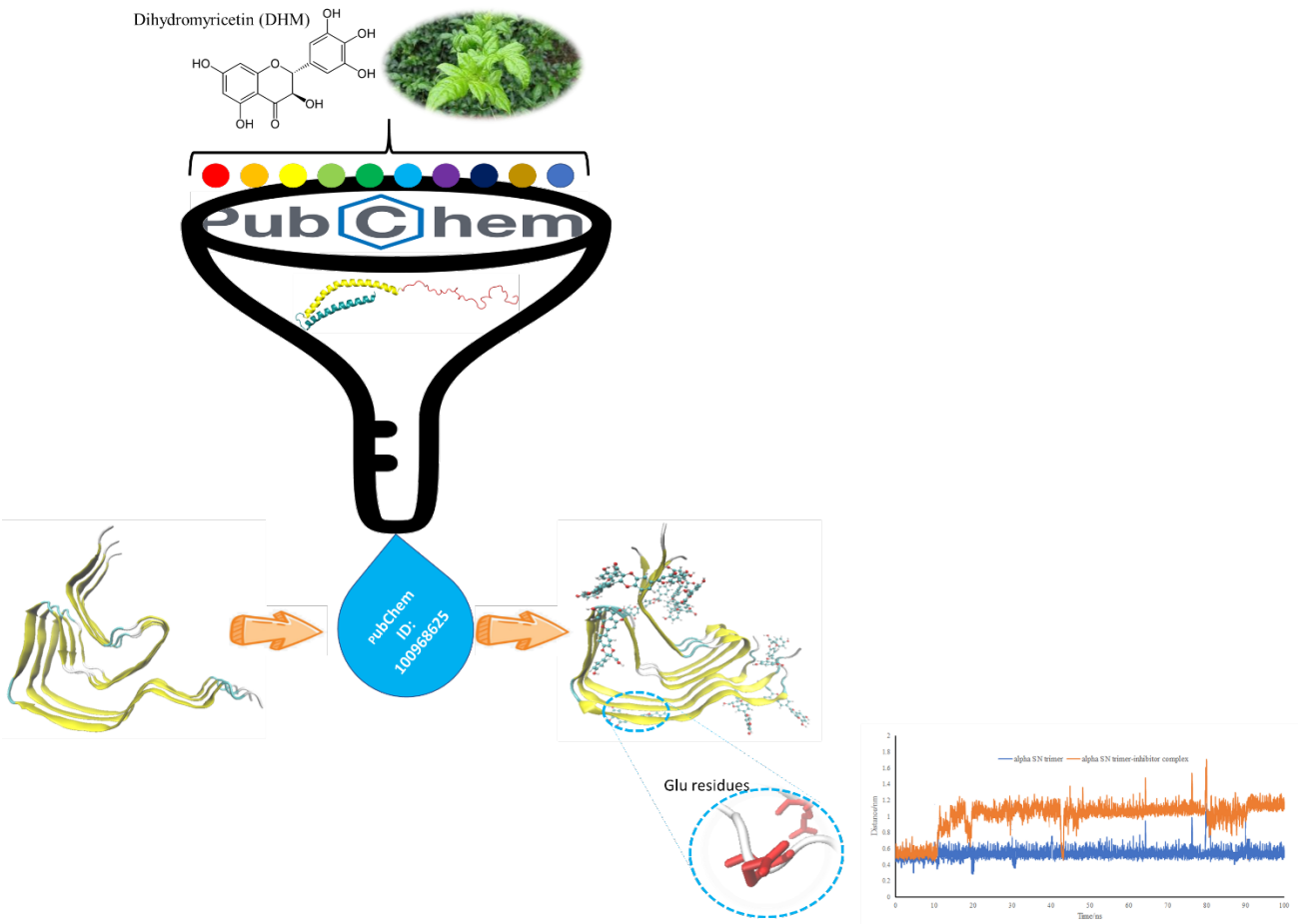
15

16

17

18

Graphical abstract:



Highlights:

- Similar compounds to DHM were selected from PubChem library using VS method.
- α SN monomer binding affinity of the filtered molecules were analyzed in details.
- The best compound was selected as α SN aggregation Inhibitor for further analysis.
- MD simulation study showed that the inhibitor weakens the structure of α SN trimer.

Abstract

Abnormal aggregation and accumulation of alpha-synuclein (α SN) in existing neurons is associated with Parkinson's disease (PD) as one of the age-related neurodegenerative disorders. Inhibition of α SN fibrillogenesis could be considered as a solution for PD diseases treatment. Here, virtual screening (VS) approach was used to investigate available ligands in PubChem library with structural similarity with Dihydromyricetin (DHM) (as a recently introduced suitable candidate for designing of novel antiPD drugs) against aggregation of α SN chains. Primary screening identified 314 promising molecules for α SN monomer, which were further analyzed in details by their binding energy and binding modes through molecular docking method. Evidently, the compound with PubChem ID of 100968625 displayed the lowest free binding energy with $\Delta G^0 = -7.1 \text{ kcal.mol}^{-1}$ and was selected for further analysis using molecular dynamics (MD) simulation method. Analysis of MD trajectories showed that molecules of the selected ligand interact with α SN trimer via H-bond interaction and destabilize the compact structure of α SN trimer. Further, prompt *in vivo* testing to validate the antiPD inhibition efficiency by this molecule can save lives.

Keywords: Parkinson disease, α -Synuclein, Dihydromyricetin, Virtual screening, MD simulation.

1. Introduction

One of the age-related neurodegenerative disorders is Parkinson's disease (PD) of which the frequency increases with the increase in age. About 2–3% of people over 65 years old worldwide suffer from the disease [1]. This disease is characterized by occurrence of Lewy bodies (LBs) which is formed by abnormal aggregation and accumulation of alpha-synuclein (α SN) in existing neurons [2, 3]. α SN is a 140 amino acids protein (molecular weight of about 14 kDa) with significant conformational flexibility that can adopt a wide range of structural conformations such as fibrils and oligomers [4, 5]. The native structure of α SN is not still exactly defined and has been described as intrinsically disordered protein (IDP) [6, 7], helical [8, 9], or a mixture of both [10]. While the function of α SN is unclear, it is highly enriched in neurons, where it is present in the presynaptic cleft as well as mitochondrial membranes. As for Alzheimer's disease (AD), for which certain oligomers of the amyloidogenic protein are toxic, the initiation of formation of α SN aggregate is suspected to be a key step in PD disease formation [11]. The cytotoxic effect of these aggregates could be because of their effect on lipid membrane permeabilisation, mitochondrial damage and oxidative stress [12]. Also, recent experimental studies have shown that the injection of α SN aggregates in animal's brain can stimulate their prion-like spread in other brain regions [13]. Most of the available drugs for PD are chemicals acting as a prodrug that will be converted in dopamine in the brain [14, 15] or are dopamine agonists inhibiting the enzymes responsible of dopamine metabolism [16, 17]. Both of these sorts of medicines cause unwanted side effects such as headaches, nausea, somnolence and so on [17]. Hence, inhibition of α SN fibrillogenesis and disaggregation of α SN fibrils by therapeutic medications could provide a more significant neuroprotective effect against PD diseases [18, 19]. Nowadays, finding of compounds that can work as robust inhibitors of α SN fibrillogenesis remains an important challenge. Given the

enormous set of existing compounds, it is impossible to perform experimental screening of all available databases in a reasonable timeframe. Advances in computational chemistry provide new opportunities to steer experiments with realistic simulations on how the available compounds may be manipulated to introduce new effective inhibitor for α SN aggregation at minimum cost.

Virtual screening (VS) is known as one of the effective methods to recognize novel bioactive compounds and is being used in many drug discovery and development strategies at the moment. In this method, the chemical entities of big libraries are rapidly screened to achieve structures with better ligand-receptor interaction pattern. In most of the VS strategies docking methods are applied on the large databases [20, 21].

Flavonoids are one of the large class of natural compounds that are mainly found in plant-derived materials and display antioxidant [22, 23] and anti-carcinogenic activities [24-26]. The ability of flavonoids to bind to carrier proteins [27-29] as well as their effects against cancer [30] and nicotine-induced oxidative stress [31] have been validated by a large number of investigations. Dihydromyricetin (DHM; Figure S1) is a flavonoid compound isolated from *Ampelopsis grossedentata* (a traditional southern Chinese herb), that has several physiological and pharmacological effects [32]. Especially, DHM showed neuroprotective against oxidative stress and valuable effects in neurodegenerative diseases [33]. Recently, Jia et. al. found that DHM could inhibit α SN fibrillogenesis and destabilize mature α SN fibrils in a dose-dependent manner [34]. Their findings suggested that DHM has a great potential to be developed into a new aggregation inhibitor for α SN. Since DHM inhibits α SN fibrillogenesis and destabilizes mature α SN fibrils, its derivatives would be suitable candidates for designing of novel antiPD drugs with inhibitory effects on aggregation of α SN.

Therefore, in the present work the following computational studies have been done to design new α SN aggregation inhibitor using VS strategy:

- 1- More than 8600 compounds with similar chemical structure to DHM were chosen from PubChem free database [35].
- 2- These compounds have been filtered on basis of Lipinski's "Rule of five" and topological polar surface area (TPSA)
- 3- The binding properties of the 314 remained compounds with α SN monomer have been investigated using molecular docking tools.
- 4- By considering the results of the VS part, the compound with lowest binding energy was chosen to perform a 100 ns molecular dynamics (MD) simulation of its complex with a α SN trimer to investigate its effect as potential inhibitor for α SN aggregation.

2. Computational procedures

2.1. Building a library of the drug-like compounds

Structure based VS is one of the common techniques being used in primary phases of drug design, discovery and development at pharmaceutical companies and academic groups [36]. To build a library of candidate molecules, the structure of DHM was selected as template and similar structures were saved from PubChem free database. The physicochemical characteristics of small molecular drugs have an important effect on their Blood-Brain barrier (BBB) permeability. Based on Lipinski's rule of five, a small molecular drug must have less than 5 H-bond donors, less than 10 H-bond acceptors, be smaller than 500 Da of molecular weight, and its calculated octanol-water partition coefficient ($\log P$) should be less than 5 to have an appropriate BBB permeability [37]. The $\log P$ value of a compound is the logarithm of its partition coefficient between n-octanol and

water ($\log (c_{\text{octanol}}/c_{\text{water}})$) and is an extent of the compound's hydrophilicity. The ideal range for BBB permeability has been found to be 1.5-2.5 [38]. We used the Lipinski's rule of five from the filters available in the PubChem database to select the candidate molecules for the VS. Then, the topological polar surface area (TPSA; as a commonly used medicinal chemistry metric for the optimization of a drug's ability to permeate cells) was calculated using Molinspiration webserver (www.molinspiration.com). Therefore, only compounds with TPSA between 20 and 130 Å² were kept in the VS database [39]. DHM and 314 other ligands met the criteria.

2.2. Molecular Docking

The experimental structure of α SN saved from PDB (PDB ID: 1XQ8) database [40]. This structure has been obtained by average structure criteria using solution NMR method. The water molecules of the .pdb file were removed and hydrogen atoms, charges, standard bond orders and the missing residues were added using Build/Check/Repair model wizard in WHAT IF web interface [41]. Minimization was carried out up to 500 steps by steepest descent method using GROMACS 2018 package [42] with GROMOS96 53A6 force field [43]. The structures of the obtained drug-like compounds were saved in .sdf format and converted to .pdbqt format using PyRx 0.8 software as input files for VS [44]. The chemical structure of DHM and the 314 other ligands (obtained after filtration by Lipinski's rule of five and TPSA calculations) were geometry optimized by AM1 semi empirical level of theory using Gaussian 09 quantum chemistry package [45] and are represented in Table S1. The blind molecular docking of DHM to α SN monomer was carried out using AutoDock Vina [46] which is an academic-free molecular docking (and virtual screening) software and works based on empirical scoring functions. The molecular docking was done based on a semi-flexible docking mechanism with a rigid receptor and flexible ligand. The default parameters were assigned for molecular docking calculations and the pose with the lowest binding energy was

chosen as final result. For the other compounds obtained from PubChem database, the center of the docking box was set in the center of the DHM binding site and the same procedure was done.

2.3.MD simulation

The initial structure of α SN trimer used in the MD simulation has been obtained from its available amyloid fibril structure determined by cryo-electron microscopy (PDB ID: 6A6B [47]). All MD simulations were performed using the GROMACS 2018 package [42] with GROMOS96 53A6 force field [43]. The force field parameters of the selected ligand (the small molecule with the most negative binding energy to α SN monomer) were obtained from prodrgr web server [48] and Lemkul's method [49] was used to correct the atomic partial charges. The α SN trimer was put in a cubic box with periodic boundary conditions (PBC) in three directions. The protein trimer was placed in the center of the box and the minimum distance between solute surface and the box was set to 1.0 nm. Ten molecules of the selected ligand were randomly placed around the α SN trimer. Then, the box was filled with SPC water molecules [50] and the system was neutralized by replacing six water molecules with Chloride ions (Cl^-). In parallel, a system of α SN trimer without the ligand molecules was also prepared. The systems were energy minimized using 50000 steps of the steepest descent method and were equilibrated for 1 ns in NVT followed by 1 ns in NPT ensembles. Finally, a 100 ns MD simulation was carried out at 1 bar and 300 K for each system. Berendsen thermostat [51] Parrinello–Rahman barostat [52, 53] and 1 nm cutoff for van der Waals (vdW) and Coulomb interactions were applied. Also, the long-range electrostatics were considered by particle mesh Ewald (PME) method [54, 55] and the equations of motion were integrated by leap-frog algorithm with a time step of 2 fs. Finally, the atomic coordinates were recorded to the trajectory file every 0.5 ps for later analysis.

3. Results and Discussion

3.1. Virtual screening and molecular docking

Considering the structural similarity with DHM as a representative inhibitor for α SN aggregation, 8609 compounds were obtained from PubChem database. The obtained compounds were filtered using Lipinski's rule of five considering their Hydrogen bonding capacity, molecular weight, and calculated log P as well as good TPSA. Finally, 314 out of 8609 compounds were selected as potential satisfied drug with possibility of good absorption or permeability through the BBB.

The previously published experimental results suggest that IDPs remain disordered in their bound state [56]. Hence, the α SN monomer was chosen to investigate its affinity for DHM binding. A molecular docking study was carried out to find out the preferred location and conformation of DHM on α SN monomer. The docking pose of the most stable DHM- α SN complex is represented in Figure 1. The results reveal that DHM binds to the terminal part of α SN monomer's IDP domain which is the α SN binding site for rosmarinic acid [57]. The standard binding free energy (ΔG^0) of this interaction is about $-5.8 \text{ kcal.mol}^{-1}$. The molecular complex system shows six H-bond interactions between DHM and Glu126, Met127, Pro128 and Glu130 residues of α SN. These H-bond interactions accompanied by hydrophobic interactions may have key roles in the stability of the system.

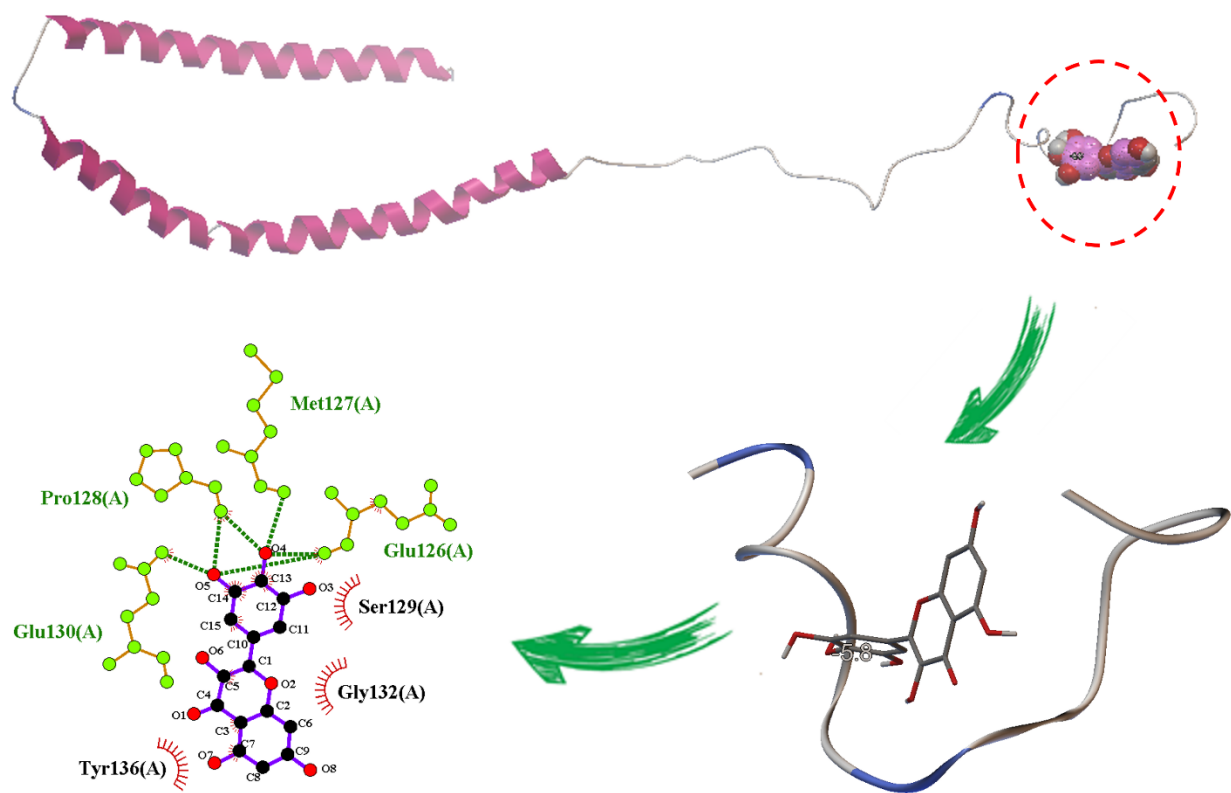


Figure 1. Docking pose of α SN-DHM complex. H-bond and hydrophobic interactions are represented as green dashed lines and red curves, respectively.

Then, 314 compounds that passed the Lipinski's rule of five and TPSA filtering were subjected to molecular docking (Table S1). These molecules were docked to the DHM binding site of α SN monomer. Achieved docked poses for each compound were ranked by their binding energies and conformations with the most negative binding energy were selected as main binding pose. Results revealed that 61 compounds among them showed lower binding energies than DHM. These compounds were highlighted in Table S1. The compound with PubChem ID 100968625 (IUPAC name: 5,7-dihydroxy-2-[(2R,3R)-3-(hydroxymethyl)-2-(4-hydroxyphenyl)-2,3-dihydro-1,4-benzodioxin-6-yl]chromen-4-one, Figure S2) displayed the lowest binding free energy ($\Delta G^0 = -7.1 \text{ kcal.mol}^{-1}$) and was selected for further analysis. The value of calculated binding free energy

is very close to the obtained values for polyphenols of *Ocimum sanctum* (OS) extract which its inhibitory effect on α SN aggregation has been studied, before [57].

Moreover, the calculated log *P* value of this molecule is about 2.4 that makes it as a good BBB permeable drug. Figure 2 represents the docking pose of the most stable complex of the selected ligand and α SN monomer. Analysis of the docking results reveals that there are three H-bond interactions between the ligand and Glu126, Pro128 and Ser129 residues of α SN. All binding energies and key residues involved in the interactions of DHM, candidate molecule and the other first 21 screened compounds with the highest binding energies, with α SN monomer are summarized in Table 1. These results revealed that H-bond, hydrophobic and π - π interactions have dominant roles in binding of candidate molecules to α SN monomer.

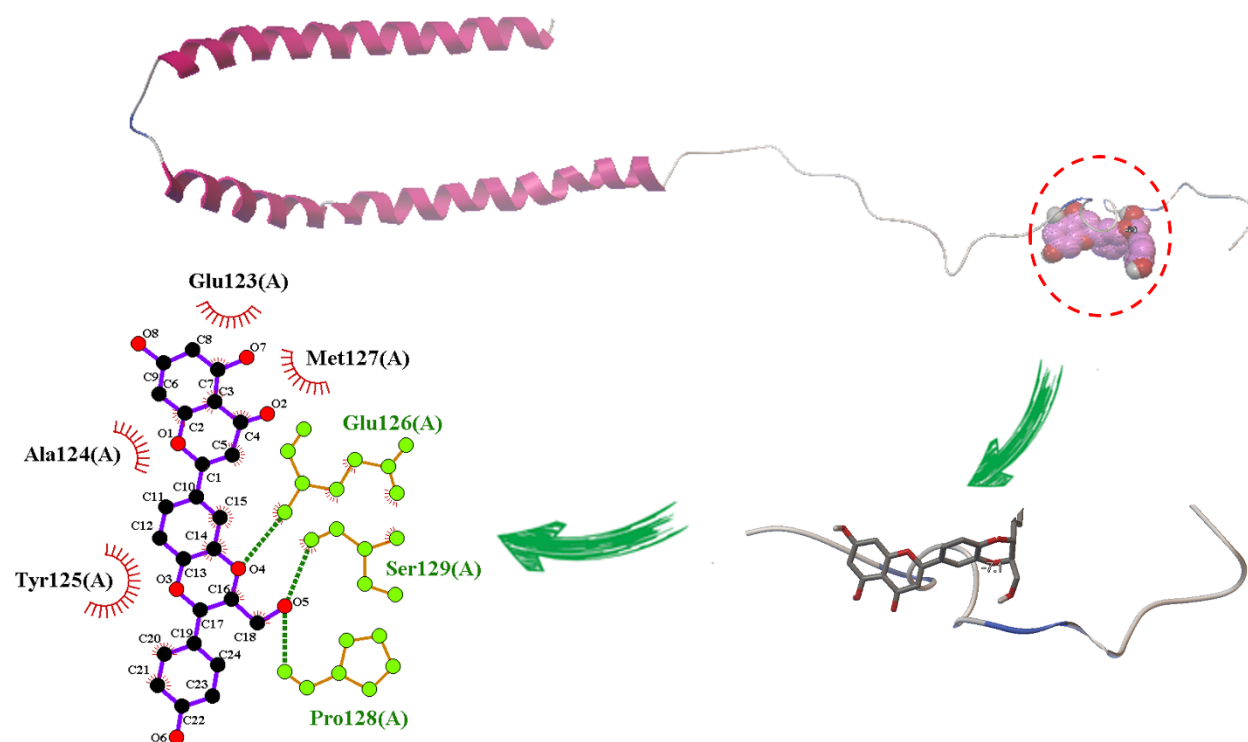


Figure 2. Docking pose of the most stable complex of the selected ligand and α SN monomer. H-bond and hydrophobic interactions are represented as green dashed lines and red curves, respectively.

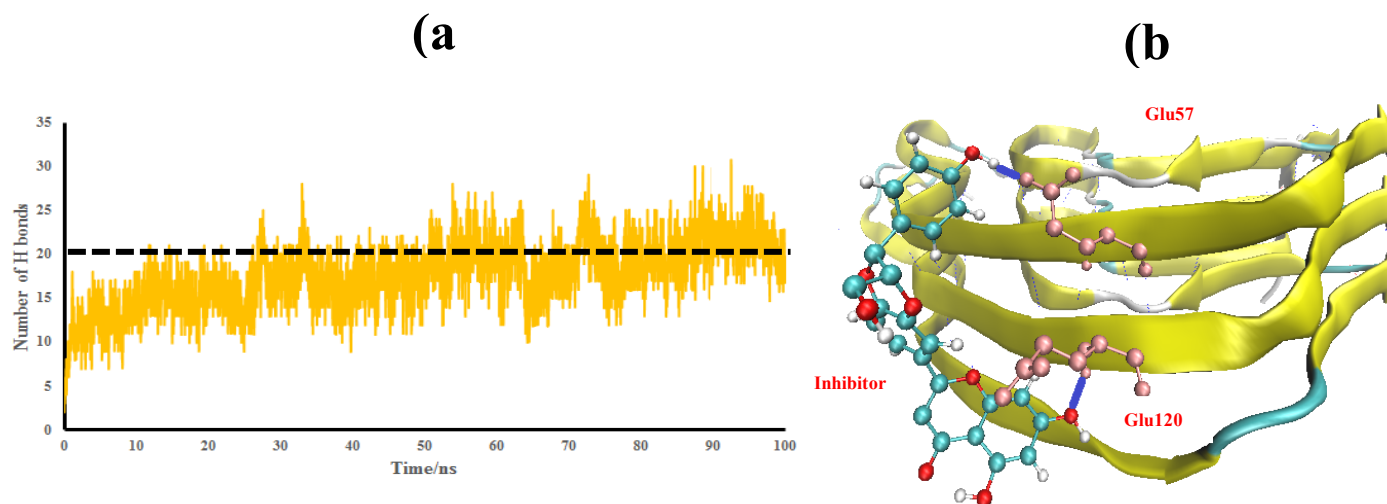
Table 1. Binding energies and key residues involved in the interactions of DHM (and the first 22 screened compounds with the highest binding energies) and α SN monomer.

Rank	Name or PubChem ID	Binding Energy/kcal.mol ⁻¹	Residues involved in:		
			H-bond interactions	Hydrophobic interactions	π - π interactions
-	DHM	-5.8	Glu126, Met127, Pro128, Glu130	Gly 132, Tyr 136	-
1	100968625	-7.1	Glu126, Pro128, Ser129	Glu 123, Ala 124, Tyr 125, Met 127	-
2	6280229	-7.0	Glu 126	Tyr 125, Met 127, Ser 129, Glu 130, Gly 132, Ala 140	Tyr 136
3	129825792	-6.9	Glu 126	Ser 129, Gly 132, Ala 140	Tyr 125, Tyr 136
4	129905005	-6.8	Glu 126, Met 127	Ser 129, Glu 130, Gly 132, Tyr 136	Tyr 125
5	5315126	-6.7	Glu 126, Pro 128	Tyr 125, Glu 130, Glu 131, Gly 132, Tyr 136	-
5	5467201	-6.7	Glu 126	Met 127	Tyr 125, Tyr 136
5	71313853	-6.7	-	Glu 126, Pro 128, Glu 130	Tyr 125
5	90643991	-6.7	Pro 128	Glu 126, Glu 130, Glu 131, Gly 132, Tyr 136	-
6	14427462	-6.5	Glu 126, Tyr 136	Tyr 125, Glu 126, Met 127, Pro 128, Glu 130, Gly 132	Tyr 136
6	67984060	-6.5	-	Glu 123, Glu 126, Pro 128, Ser 129	-
6	90643985	-6.5	Met 127	Glu 126, Ser 129, Glu 130, Gly 132, Tyr 136	Tyr 125
6	90643986	-6.5	-	Glu 126, Gly 132, Tyr 136	Tyr 125
6	90643987	-6.5	Glu 126	Tyr 125, Ser 129, Gly 132, Tyr 136	-
6	129825797	-6.5	Glu 126	Ser 129, Glu 130, Gly 132, Tyr 136	-
6	129904975	-6.5	Met 127	Glu 126, Ser 129, Glu 130, Gly 132, Tyr 136	Tyr 125
7	5315125	-6.4	Glu 126	Tyr 125, Glu 130, Gly 132, Tyr 136	-
7	14427460	-6.4	Pro 128	Tyr 125, Met 127, Glu 130, Glu 131, Gly 132	Tyr 136
7	23630406	-6.4	-	Glu 126, Ser 129, Glu 130, Glu 131, Tyr 136	-
8	580166	-6.3	-	Glu 126, Ser 129, Glu 131	Tyr 125
8	13349170	-6.3	-	Tyr 125	-
8	13834128	-6.3	Met 127	Tyr 125, Glu 126, Pro 128, Glu 131	-
8	18542127	-6.3	-	Tyr 125, Glu 126, Glu 130, Gly 132, Asp 135	-

3.2.MD simulation

The interactions between ten molecules of the selected ligand (PubChem ID: 100968625) and a α SN trimer was investigated using MD simulations method. The selected ligand (Figure S2) contains a carbonyl group, two ether oxygen atoms, and five hydroxyl groups that can interact with α SN via H-bond interaction. This makes a total of 8 possible H-bond sites for each ligand molecule. Therefore, the total number of H-bonds formed between the α SN trimer and the ten ligand molecules was calculated and shown in Figure 3. Analysis of the results showed that H-bonds were formed between the α SN trimer and ligands, rapidly after few ns of MD simulation trajectory and their number increased to about 20 at around 30 ns and fluctuated around this mean value until the end (about 2 H-bonds per ligand molecule). Figure 3b shows the representative

1 structure of α SN and one of the ligands molecules interacting by H-bond interactions. It shows
 2 that there was a H-bond interaction between hydrogen atom of the hydroxyl group of the ligand
 3 and an oxygen atom of the carboxyl group of the side chain of the residue Glu57. Same interaction
 4 has been reported for the interaction of DHM molecules with α SN trimer [34]. At the same time,
 5 there was another hydrogen bond between the same ligand and the amide group of residue Glu120.



6 **Figure 3.** Interaction of the selected ligand (PubChem ID: 100968625) with the α SN trimer. (a) Total number of
 7 hydrogen bonds between the α SN trimer and the ten ligand molecules during 100 ns of MD simulation. (b) Binding
 8 conformation between residues in the α SN trimer and one of the ligand molecules at the end of trajectory. The blue
 9 solid lines represent the H-bonds. Glu residues have been shown as pink ball & stick representation.

10
 11 This observation is completely in agreement with the docking results and proves the key role of
 12 H-bond interactions in the stability of inhibitor- α SN complex. Furthermore, the previously
 13 published results have confirmed that H-bond interactions have important role in the interaction
 14 of their suggested inhibitors and α SN protein [21, 34, 57, 58]. The compactness of α SN trimer
 15 during the MD simulations (in the presence and absence of the selected compound) is an important
 16 factor to study the inhibitory effect of the candidate drug and conformational changes of the protein
 17 trimer during its interaction with it. Therefore, the radius of gyration (R_g) of the α SN trimer was

evaluated as an index of protein structural compactness. Figure 4 shows that the R_g of α SN trimer in the presence of the selected compound increased in comparison to the case without the compound indicating the less compact structure of α SN trimer (Figure 4). The average values of R_g are about 2.03 and 2.11 nm for free α SN and its complex with 10 molecules of the candidate drug, respectively. This observation proves that the compound destabilizes the compact structure of α SN trimer.

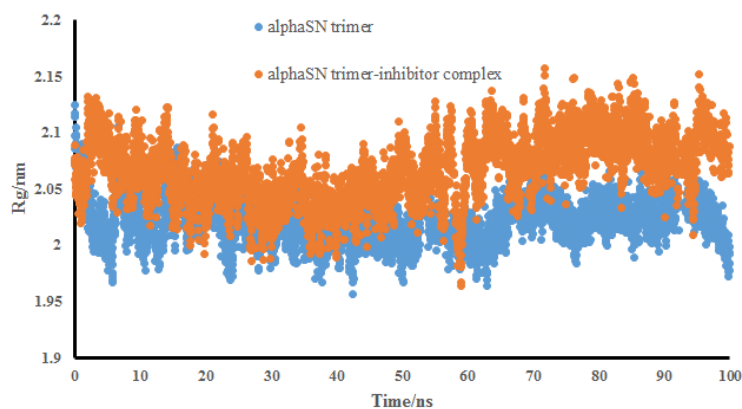


Figure 4. Time dependence of the radius of gyration (R_g) for α SN trimer during the simulation, in the absence and presence of inhibitor.

To evaluate the mobility of the residues of α SN trimer, the root mean square fluctuations (RMSF) of the residues of protein aggregate in the absence and presence of inhibitor were analyzed and presented in Figure 5.

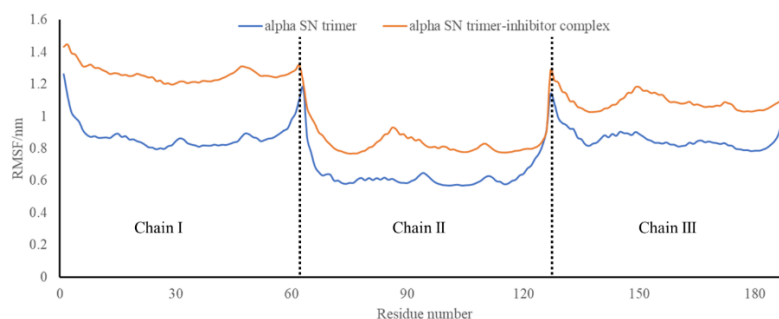


Figure 5. RMSF values of residues of α SN trimer during the 100 ns of simulation time, in the absence and presence of the inhibitor. (Chain I: residues 1-63; Chain II: residues 64-126 and Chain III: residues 127-189).

The results of the RMSF analysis indicate that all the residues of α SN trimer show higher fluctuations in the presence of inhibitor molecules in comparison to the state without inhibitors. This observation is in consistency with the R_g results and could be another evidence about good inhibitory effect of the selected compound as new inhibitor of α SN aggregation. The middle chain (chain II in figure 5) of the α SN trimer has been surrounded between two other chains and is not accessible for the inhibitor molecules as much as two other chains. This protection causes its less fluctuations in comparison to the chains I and III of the protein trimer in both states (in the presence and absence of the inhibitors).

Figure 6 represents that during 100 ns of MD simulation trajectory, most of the inhibitor molecules associate in N-terminal of the protein trimer that causes higher fluctuation of this part in three chains of α SN trimer as it is clear in Figure 5. In the presence of the inhibitor, the N-terminal fluctuations of the three chains are about 14%, 15% and 18% higher than C-terminal for Chains I to III, respectively. However, the maximum RMSF difference between the N- and C-terminal in the absence of the inhibitor would be only about 7% (for chain I). In other words, the interaction of inhibitor molecules with α SN chains weakens the intermolecular interactions between the N-terminal residues of the protein trimer and increase the fluctuations of the residues in this part of

the protein. Furthermore, one inhibitor molecule inserts into the interspace between two chains of the α SN trimer, which would disturb the intermolecular interactions between the chains. To prove this claim, the distance between the C α atoms of Glu57 of chain I and Glu120 of chain II was calculated as shown in Figure 7. The average distance in the presence of inhibitor was about 12 Å after 20 ns, while the distance in the α SN trimer in water was nearly 5 Å during the entire simulation time. Therefore, insertion of the inhibitor molecule inside the inner space of the α SN chains caused a loss of contact between two chains and disrupted their initial ordered structure.

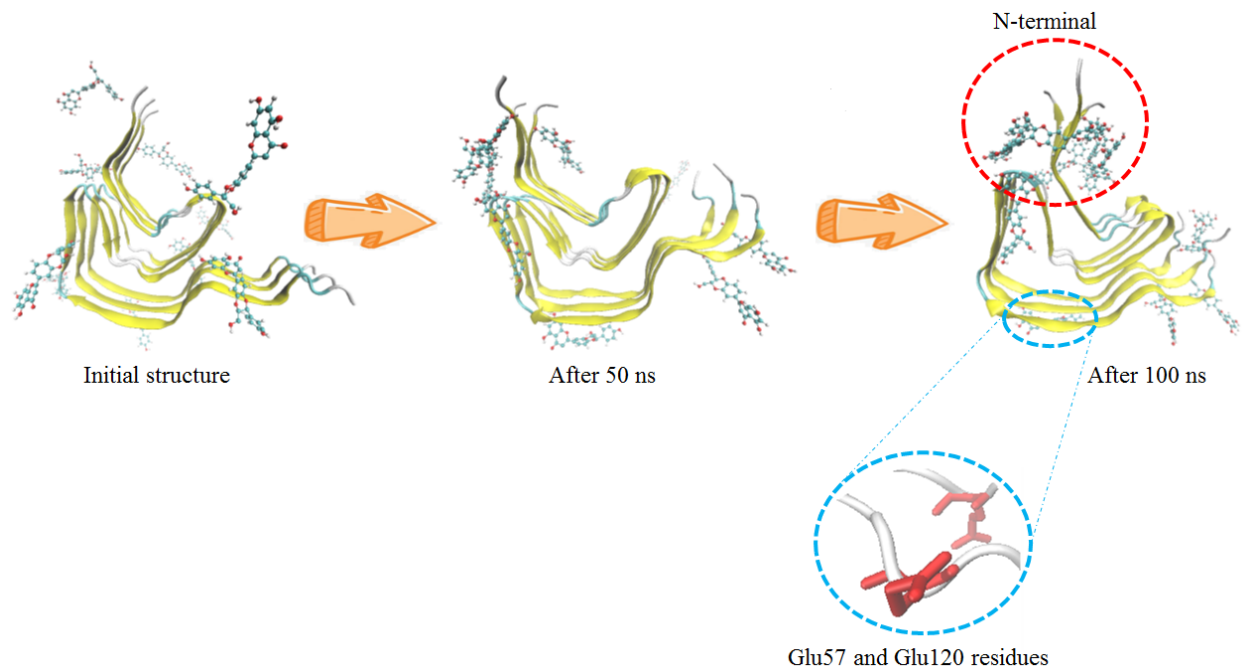


Figure 6. Configuration of the ligand molecules around α SN trimer during 100 ns of MD simulation.

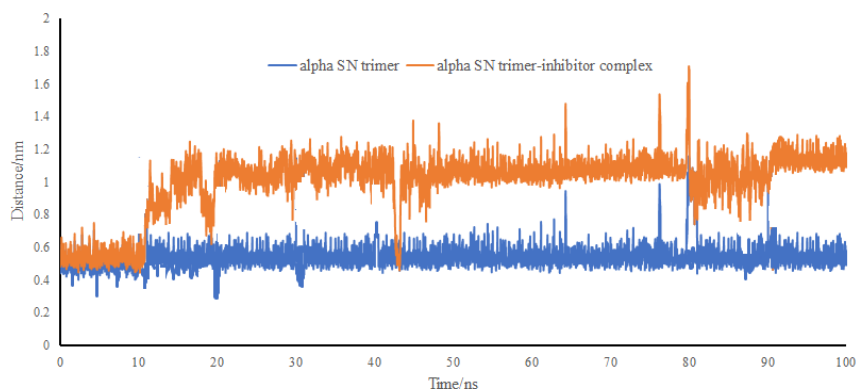


Figure 7. Change of Glu57-Glu120 distance in chains I and II of α SN trimer during the simulation, in the absence and presence of inhibitor.

4. Conclusion

In this study, we built a library of compounds with similar structure of Dihydromyricetin (DHM; a natural flavonoid with inhibitory effect on α SN fibrillogenesis). Lipinski's "Rule of five" and TPSA screenings were used to select the drug like compounds. Moreover, binding free energy and binding modes of the filtered compounds were investigated using in silico virtual screening method. The analysis of the molecular docking calculations showed that the compound with PubChem ID of 100968625 has the highest affinity for binding to α SN monomer ($\Delta G^0_{\text{binding}} = -7.1$ kcal.mol⁻¹) among the other candidates. Its high binding affinity for α SN suggested that this compound could be considered as an inhibitor for α SN aggregation with higher efficiency than DHM and some of the other previously suggested antiPD drugs. The behavior of α SN trimer in the presence of the selected candidate was further analyzed using molecular dynamics (MD) simulation method. Analysis of MD trajectories showed that H-bond interactions between the hydroxyl groups of the ligand molecules with side chains of the residues in α SN trimer could destabilize the compact structure of α SN trimer. On the other hand, most of the inhibitor molecules

1 associate in N-terminal of the protein trimer and cause 100% increasing of fluctuations for the
2 residues in N-terminal of the trimer structure. Also, investigation of R_g of the α SN trimer showed
3 that the inhibitor molecules decrease the compactness of protein structure for about 4% in
4 comparison to the protein free state in water. Furthermore, penetration of one inhibitor molecule
5 into the interspace of two protein chains, disturbed the ordered structure of the α SN filament,
6 weakened the intermolecular interactions between the protein chains and increased their distance.
7 In conclusion, our study revealed the inhibitory effect of selected ligand (PubChem
8 ID=100968625) on α SN fibrillogenesis. Eventually, we believe that this study will shed the lights
9 on finding of potentially active compounds against the α SN aggregation. We also confirm that it
10 is necessary to do further in vitro and in vivo investigations for developing potent drug inhibitors
11 of α SN fibrillogenesis for the treatment of PD and similar diseases.

19 **Acknowledgments**

20 M.S. is grateful to the French Agence Nationale de la Recherche (Grant: ANR-BIOLUM ANR-
21 16-CE29-0013).

References:

- [1]. Poewe, W., et al., *Parkinson disease*. Nature reviews Disease primers, 2017. **3**(1): p. 1-21.DOI: <https://doi.org/10.1038/nrdp.2017.13>.
- [2]. Lewy, F.H., *Paralysis agitans. I*. Pathologische anatomie. Handbuch der neurologie, 1912.
- [3]. Xu, L. and J. Pu, *Alpha-synuclein in Parkinson's disease: from pathogenetic dysfunction to potential clinical application*. Parkinson's Disease, 2016. **2016**.DOI: <https://doi.org/10.1155/2016/1720621>.
- [4]. Deleersnijder, A., et al., *The remarkable conformational plasticity of alpha-synuclein: blessing or curse?* Trends in molecular medicine, 2013. **19**(6): p. 368-377.DOI: <https://doi.org/10.1016/j.molmed.2013.04.002>.
- [5]. Mehra, S., S. Sahay, and S.K. Maji, *α -Synuclein misfolding and aggregation: Implications in Parkinson's disease pathogenesis*. Biochimica et Biophysica Acta (BBA)-Proteins and Proteomics, 2019. **1867**(10): p. 890-908.DOI: <https://doi.org/10.1016/j.bbapap.2019.03.001>.
- [6]. Breydo, L., J.W. Wu, and V.N. Uversky, *α -Synuclein misfolding and Parkinson's disease*. Biochimica et Biophysica Acta (BBA)-Molecular Basis of Disease, 2012. **1822**(2): p. 261-285.DOI: <https://doi.org/10.1016/j.bbadis.2011.10.002>.
- [7]. Theillet, F.-X., et al., *Structural disorder of monomeric α -synuclein persists in mammalian cells*. Nature, 2016. **530**(7588): p. 45-50.DOI: <https://doi.org/10.1038/nature16531>.
- [8]. Bartels, T., J.G. Choi, and D.J. Selkoe, *α -Synuclein occurs physiologically as a helically folded tetramer that resists aggregation*. Nature, 2011. **477**(7362): p. 107-110.DOI: <https://doi.org/10.1038/nature10324>.

- [9]. Wang, W., et al., *A soluble α -synuclein construct forms a dynamic tetramer*. Proceedings of the National Academy of Sciences, 2011. **108**(43): p. 17797-17802.DOI: <https://doi.org/10.1073/pnas.1113260108>.
- [10]. Burré, J., et al., *Properties of native brain α -synuclein*. Nature, 2013. **498**(7453): p. E4-E6.DOI: <https://doi.org/10.1038/nature12125>.
- [11]. Winner, B., et al., *In vivo demonstration that α -synuclein oligomers are toxic*. Proceedings of the National Academy of Sciences, 2011. **108**(10): p. 4194-4199.DOI: <https://doi.org/10.1073/pnas.1100976108>.
- [12]. Ma, L., et al., *Non-polyphenolic natural inhibitors of amyloid aggregation*. European journal of medicinal chemistry, 2020. **192**: p. 112197.DOI: <https://doi.org/10.1016/j.ejmech.2020.112197>.
- [13]. Sangwan, S., et al., *Inhibition of synucleinopathic seeding by rationally designed inhibitors*. Elife, 2020. **9**: p. e46775.DOI: <https://doi.org/10.7554/eLife.46775>.
- [14]. Chakraborty, A., S. Brauer, and A. Diwan, *A review of possible therapies for Parkinson's disease*. Journal of Clinical Neuroscience, 2020. **76**: p. 1-4.
- [15]. Haddad, F., et al., *Dopamine and levodopa prodrugs for the treatment of Parkinson's disease*. Molecules, 2018. **23**(1): p. 40.
- [16]. Stoker, T.B., K.M. Torsney, and R.A. Barker, <https://doi.org/10.3389/fnins.2018.00693>. Frontiers in neuroscience, 2018. **12**: p. 693.
- [17]. Carrera, I. and R. Cacabelos, *Current drugs and potential future neuroprotective compounds for Parkinson's disease*. Current neuropharmacology, 2019. **17**(3): p. 295-306.

- [18]. El-Agnaf, O.M., et al., *A strategy for designing inhibitors of α -synuclein aggregation and toxicity as a novel treatment for Parkinson's disease and related disorders*. The FASEB journal, 2004. **18**(11): p. 1315-1317.DOI: <https://doi.org/10.1096/fj.03-1346fje>.
- [19]. Nagai, Y., et al., *Inhibition of polyglutamine protein aggregation and cell death by novel peptides identified by phage display screening*. Journal of Biological Chemistry, 2000. **275**(14): p. 10437-10442.DOI: <https://doi.org/10.1074/jbc.275.14.10437>.
- [20]. Vittorio, S., et al., *Rational design of small molecules able to inhibit α -synuclein amyloid aggregation for the treatment of Parkinson's disease*. Journal of Enzyme Inhibition and Medicinal Chemistry, 2020. **35**(1): p. 1727-1735.DOI: <https://doi.org/10.1080/14756366.2020.1816999>.
- [21]. Jafaripour, S.S., et al., *In silico drug repositioning of FDA-approved drugs to predict new inhibitors for alpha-synuclein aggregation*. Computational Biology and Chemistry, 2020. **88**: p. 107308.
- [22]. van Acker, F.A., et al., *Flavonoids can replace α -tocopherol as an antioxidant*. FEBS letters, 2000. **473**(2): p. 145-148.DOI: [https://doi.org/10.1016/S0014-5793\(00\)01517-9](https://doi.org/10.1016/S0014-5793(00)01517-9).
- [23]. Yu, J., et al., *Antioxidant activity of citrus limonoids, flavonoids, and coumarins*. Journal of agricultural and food chemistry, 2005. **53**(6): p. 2009-2014.DOI: <https://doi.org/10.1021/jf0484632>.
- [24]. Kawaii, S., et al., *Quantitation of flavonoid constituents in citrus fruits*. Journal of Agricultural and Food Chemistry, 1999. **47**(9): p. 3565-3571.DOI: <https://doi.org/10.1021/jf990153+>.
- [25]. Pszczola, D., *Natural colors: pigments of imagination*. Food technology (USA), 1998.

- [26]. Cooray, H.C., et al., <https://doi.org/10.1016/j.bbrc.2004.03.040>. Biochemical and biophysical research communications, 2004. **317**(1): p. 269-275.
- [27]. Khosravi, I. and M. Sahihi, *Computational Studies on the Interaction of Arctiin and Liquiritin With β -lactoglobulin*. Journal of Macromolecular Science, Part B, 2014. **53**(9): p. 1591-1600.DOI: <https://doi.org/10.1080/00222348.2014.946844>.
- [28]. Sahihi, M., *In-silico study on the interaction of saffron ligands and beta-lactoglobulin by molecular dynamics and molecular docking approach*. Journal of Macromolecular Science, Part B, 2016. **55**(1): p. 73-84.DOI: <https://doi.org/10.1080/00222348.2015.1125066>.
- [29]. Sahihi, M. and Y. Ghayeb, *Binding of biguanides to β -lactoglobulin: molecular-docking and molecular dynamics simulation studies*. Chemical Papers, 2014. **68**(11): p. 1601-1607.DOI: <https://doi.org/10.2478/s11696-014-0598-7>.
- [30]. Williams, R.J., J.P. Spencer, and C. Rice-Evans, *Flavonoids: antioxidants or signalling molecules?* Free radical biology and medicine, 2004. **36**(7): p. 838-849.DOI: <https://doi.org/10.1016/j.freeradbiomed.2004.01.001>.
- [31]. Sengupta, B., et al., *Differential roles of 3-Hydroxyflavone and 7-Hydroxyflavone against nicotine-induced oxidative stress in rat renal proximal tubule cells*. PloS one, 2017. **12**(6): p. e0179777.DOI: <https://doi.org/10.1371/journal.pone.0179777>.
- [32]. Murakami, T., et al., *Hepatoprotective activity of tocha, the stems and leaves of Ampelopsis grossedentata, and ampelopsin*. Biofactors, 2004. **21**(1-4): p. 175-178.
- [33]. Kou, X., et al., *Ampelopsin attenuates 6-OHDA-induced neurotoxicity by regulating GSK-3 β /NRF2/ARE signalling*. Journal of functional foods, 2015. **19**: p. 765-774.DOI: <https://doi.org/10.1016/j.jff.2015.10.010>.

- [34]. Jia, L., et al., *Dihydromyricetin Inhibits α -Synuclein Aggregation, Disrupts Preformed Fibrils, and Protects Neuronal Cells in Culture against Amyloid-Induced Cytotoxicity*. Journal of agricultural and food chemistry, 2019. **67**(14): p. 3946-3955.DOI: <https://doi.org/10.1021/acs.jafc.9b00922>.
- [35]. Kim, S., et al., *PubChem 2019 update: improved access to chemical data*. Nucleic acids research, 2019. **47**(D1): p. D1102-D1109.DOI: <https://doi.org/10.1093/nar/gky1033>.
- [36]. Mirza, S.B., et al., *Discovery of selective dengue virus inhibitors using combination of molecular fingerprint-based virtual screening protocols, structure-based pharmacophore model development, molecular dynamics simulations and in vitro studies*. Journal of Molecular Graphics and Modelling, 2018. **79**: p. 88-102.DOI: <https://doi.org/10.1016/j.jmgm.2017.10.010>.
- [37]. Lipinski, C.A., et al., *Experimental and computational approaches to estimate solubility and permeability in drug discovery and development settings*. Advanced drug delivery reviews, 1997. **23**(1-3): p. 3-25.DOI: [https://doi.org/10.1016/S0169-409X\(96\)00423-1](https://doi.org/10.1016/S0169-409X(96)00423-1).
- [38]. Mikitsh, J.L. and A.-M. Chacko, *Pathways for small molecule delivery to the central nervous system across the blood-brain barrier*. Perspectives in medicinal chemistry, 2014. **6**: p. PMC. S13384.DOI: <https://doi.org/10.4137%2FPMC.S13384>.
- [39]. Jin, Z., et al., *Structure-based virtual screening of influenza virus RNA polymerase inhibitors from natural compounds: molecular dynamics simulation and MM-GBSA calculation*. Computational biology and chemistry, 2020. **85**: p. 107241.
- [40]. Ulmer, T.S., et al., *Structure and dynamics of micelle-bound human α -synuclein*. Journal of Biological Chemistry, 2005. **280**(10): p. 9595-9603.DOI: <https://doi.org/10.1074/jbc.M411805200>.

- [41]. Vriend, G., *WHAT IF: a molecular modeling and drug design program*. Journal of molecular graphics, 1990. **8**(1): p. 52-56.DOI: [https://doi.org/10.1016/0263-7855\(90\)80070-V](https://doi.org/10.1016/0263-7855(90)80070-V).
- [42]. Berendsen, H.J., D. van der Spoel, and R. van Drunen, *GROMACS: a message-passing parallel molecular dynamics implementation*. Computer physics communications, 1995. **91**(1-3): p. 43-56.DOI: [https://doi.org/10.1016/0010-4655\(95\)00042-E](https://doi.org/10.1016/0010-4655(95)00042-E).
- [43]. Oostenbrink, C., et al., *A biomolecular force field based on the free enthalpy of hydration and solvation: the GROMOS force-field parameter sets 53A5 and 53A6*. Journal of computational chemistry, 2004. **25**(13): p. 1656-1676.DOI: <https://doi.org/10.1002/jcc.20090>.
- [44]. Dallakyan, S. and A.J. Olson, *Small-molecule library screening by docking with PyRx*, in *Chemical biology*. 2015, Springer. p. 243-250.
- [45]. Frisch, M., et al., *EM64L-Gaussian 09, Revision D. 01*, Gaussian. Inc., Wallingford CT, 2013.
- [46]. Trott, O. and A.J. Olson, *AutoDock Vina: improving the speed and accuracy of docking with a new scoring function, efficient optimization, and multithreading*. Journal of computational chemistry, 2010. **31**(2): p. 455-461.DOI: <https://doi.org/10.1002/jcc.21334>.
- [47]. Li, Y., et al., *Amyloid fibril structure of α -synuclein determined by cryo-electron microscopy*. Cell research, 2018. **28**(9): p. 897-903.DOI: <https://doi.org/10.1038/s41422-018-0075-x>.
- [48]. Schüttelkopf, A.W. and D.M. Van Aalten, *PRODRG: a tool for high-throughput crystallography of protein–ligand complexes*. Acta Crystallographica Section D:

- Biological Crystallography, 2004. **60**(8): p. 1355-1363.DOI: <https://doi.org/10.1107/S0907444904011679>.
- [49]. Lemkul, J.A., W.J. Allen, and D.R. Bevan, *Practical considerations for building GROMOS-compatible small-molecule topologies*. Journal of chemical information and modeling, 2010. **50**(12): p. 2221-2235.DOI: <https://doi.org/10.1021/ci100335w>.
- [50]. Pullman, A., *Intermolecular forces*. Vol. 14. 2013: Springer Science & Business Media.
- [51]. Lemak, A. and N. Balabaev, *On the Berendsen thermostat*. Molecular Simulation, 1994. **13**(3): p. 177-187.DOI: <https://doi.org/10.1080/08927029408021981>.
- [52]. Parrinello, M. and A. Rahman, *Polymorphic transitions in single crystals: A new molecular dynamics method*. Journal of Applied physics, 1981. **52**(12): p. 7182-7190.DOI: <https://doi.org/10.1063/1.328693>.
- [53]. Rahman, A. and F.H. Stillinger, *Molecular dynamics study of liquid water*. The Journal of Chemical Physics, 1971. **55**(7): p. 3336-3359.DOI: <https://doi.org/10.1063/1.1676585>.
- [54]. Darden, T., D. York, and L. Pedersen, *Particle mesh Ewald: An $N \cdot \log(N)$ method for Ewald sums in large systems*. The Journal of chemical physics, 1993. **98**(12): p. 10089-10092.DOI: <https://doi.org/10.1063/1.464397>.
- [55]. Essmann, U., et al., *A smooth particle mesh Ewald method*. The Journal of chemical physics, 1995. **103**(19): p. 8577-8593.DOI: <https://doi.org/10.1063/1.470117>.
- [56]. Liu, Z. and Y. Huang, *Advantages of proteins being disordered*. Protein Science, 2014. **23**(5): p. 539-550.DOI: <https://doi.org/10.1002/pro.2443>.
- [57]. Meena, V.K., V. Kumar, and S. Karalia, <https://doi.org/10.1016/j.molliq.2021.116176>. Journal of Molecular Liquids, 2021. **336**: p. 116176.

1 [58]. Jayaraj, R.L. and N. Elangovan, *In silico identification of potent inhibitors of alpha-*
2 *synuclein aggregation and its in vivo evaluation using MPTP induced Parkinson mice*
3 *model*. Biomedicine & Aging Pathology, 2014. **4**(2): p. 147-152.

4

5

Supporting Information

Identification of new alpha-synuclein fibrillogenesis inhibitor using in silico structure-based virtual screening

Mehdi Sahihi^{1,2,}, Fatma Gaci², Isabelle Navizet²*

¹Roberval Laboratory, Université de Technologie de Compiègne, Alliance Sorbonne Université,
Compiègne, France

²MSME, Univ Gustave Eiffel, CNRS UMR 8208, Univ Paris Est Creteil,
F-77454 Marne-la-Vallée, France

***Corresponding author:**

Mehdi Sahihi

Tel: +33 (0) 6 24 67 38 28

Fax: +33 (0) 1 60 95 77 99

E-mail: mehdi.sahihi@gmail.com

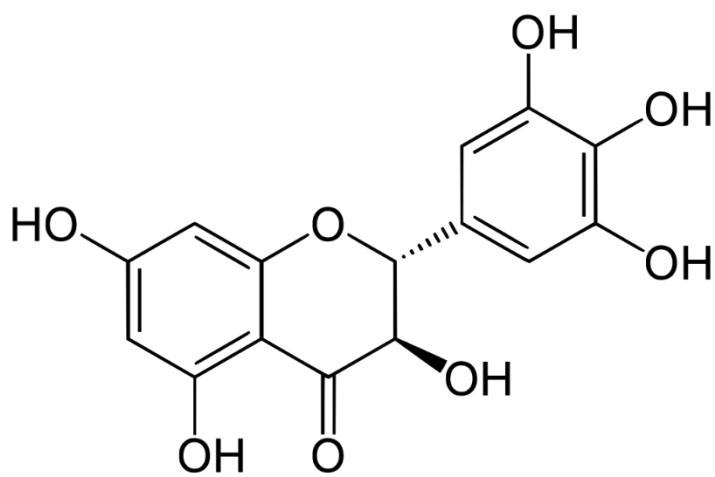


Figure S1. Chemical structure of Dihydromyricetin (DHM).

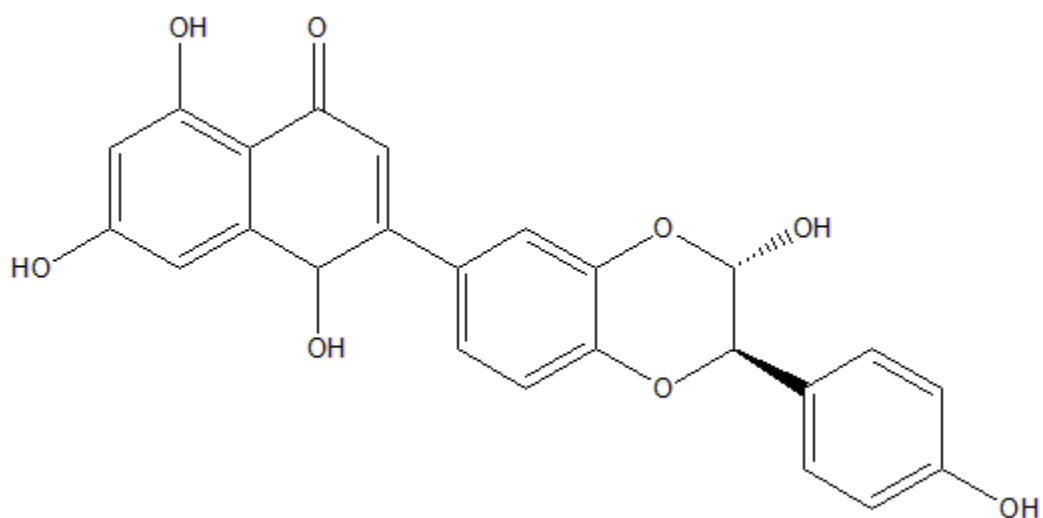
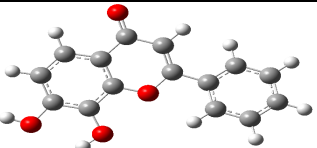
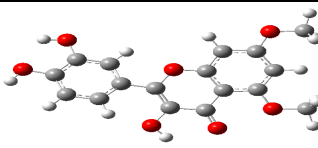
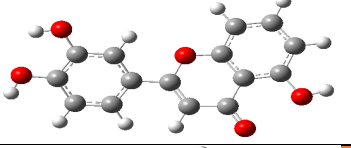
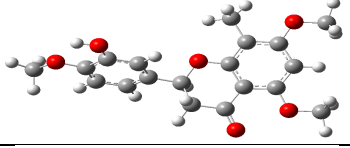
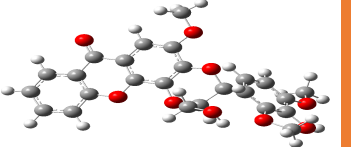
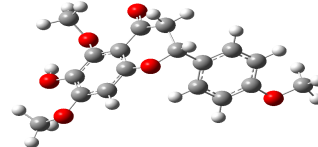
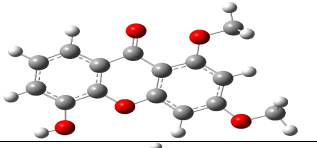
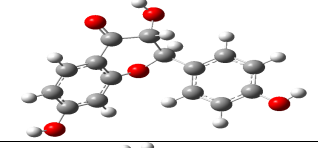
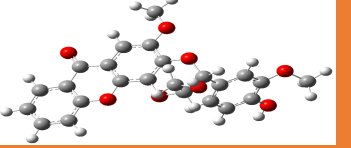
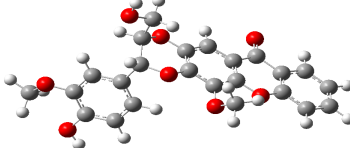
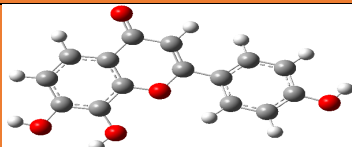
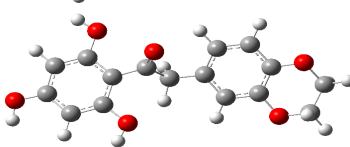
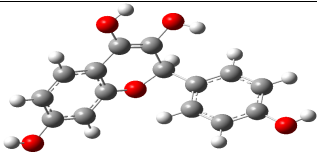
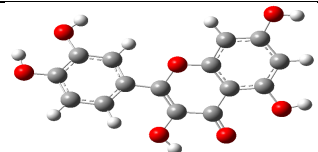
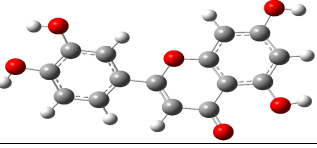
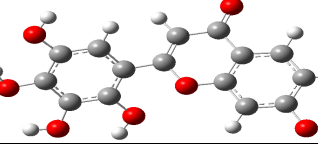
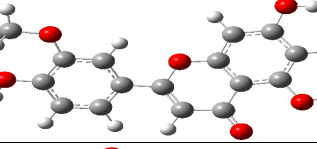
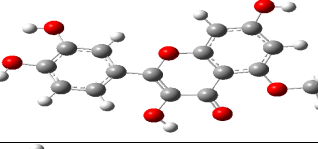
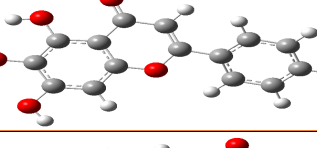
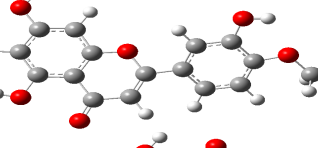
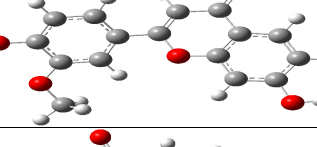
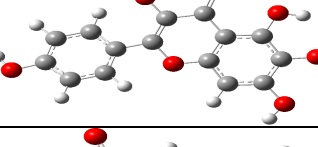
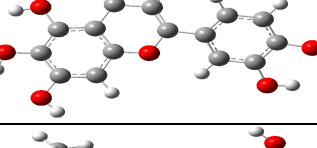
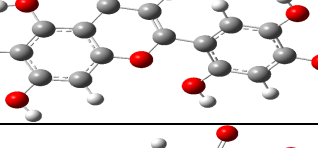
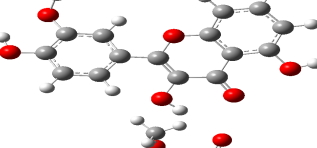
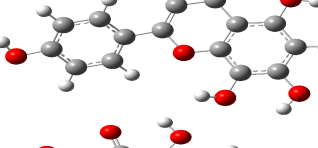
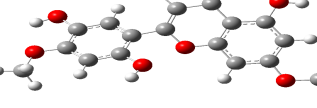
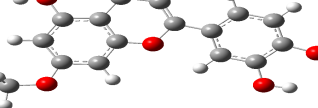
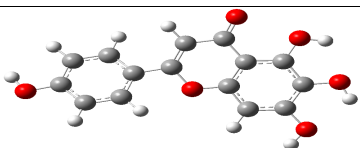
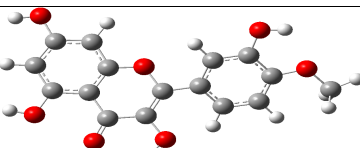
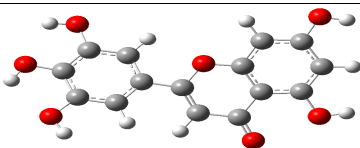
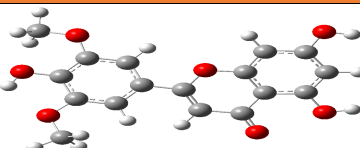
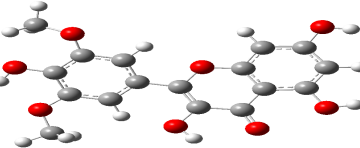
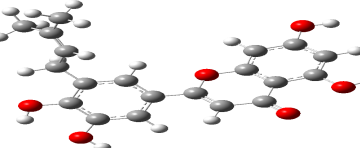
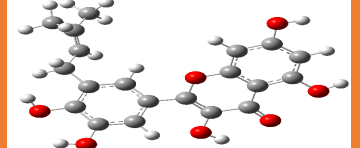
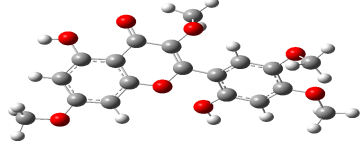
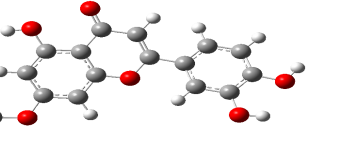
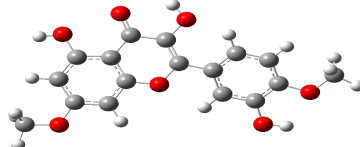
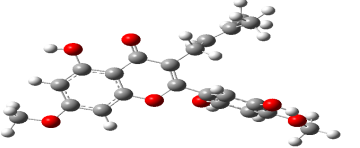
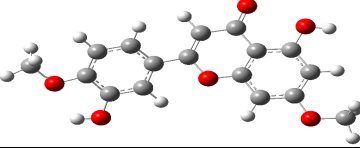
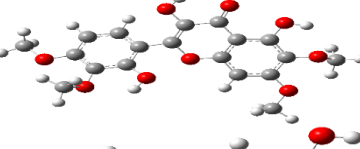
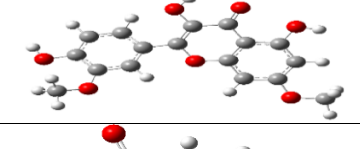
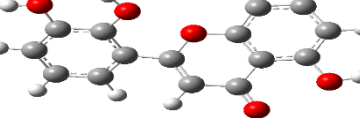
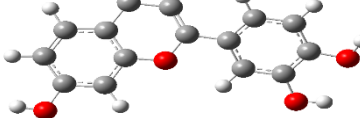


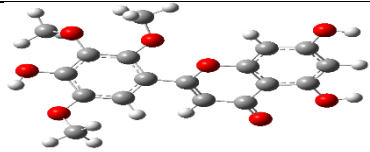
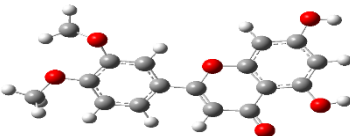
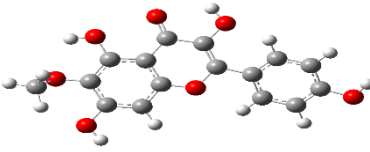
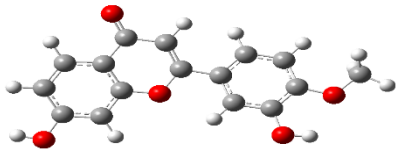
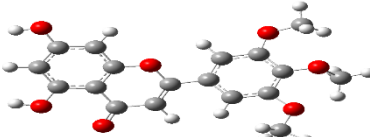
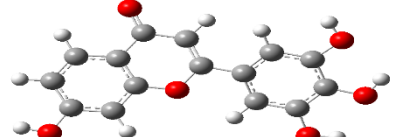
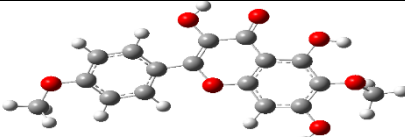
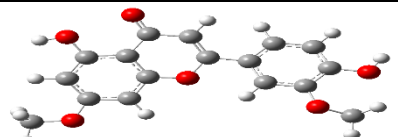
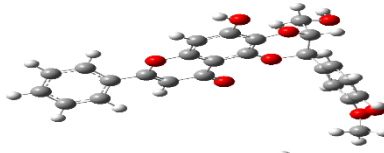
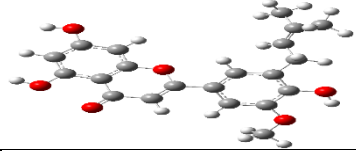
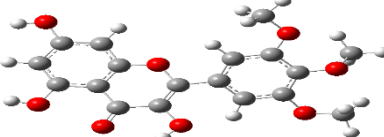
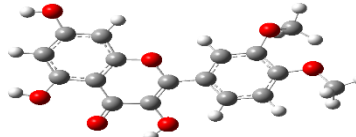
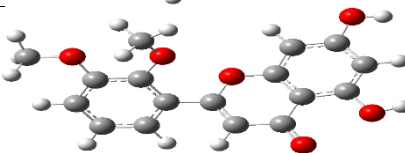
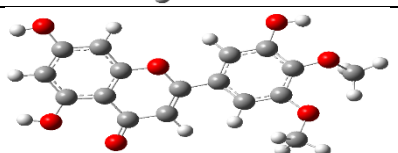
Figure S2. Chemical structure of the selected ligand from PubChem free database using virtual screening method (PubChem ID of 100968625; IUPAC name: 5,7-dihydroxy-2-[(2R,3R)-3-(hydroxymethyl)-2-(4-hydroxyphenyl)-2,3-dihydro-1,4-benzodioxin-6-yl]chromen-4-one).

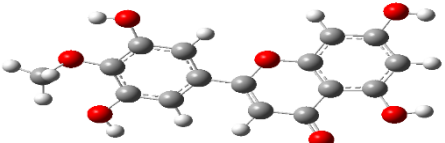
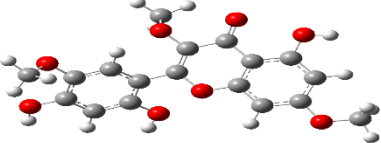
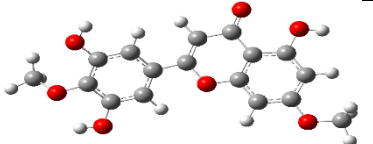
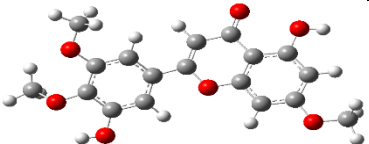
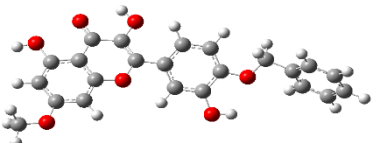
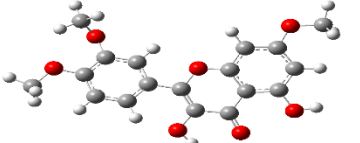
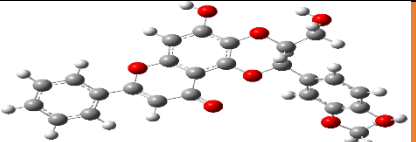
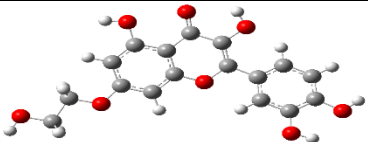
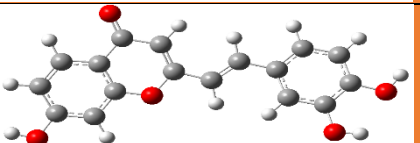
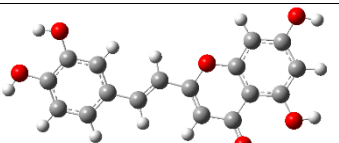
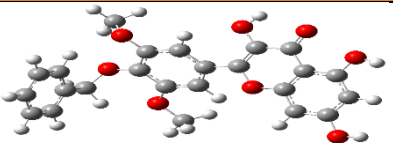
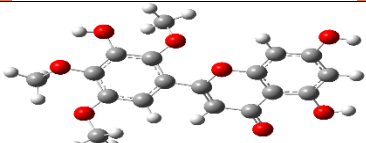
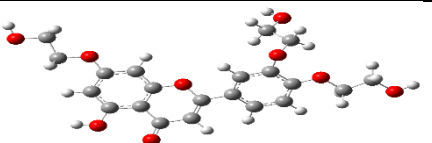
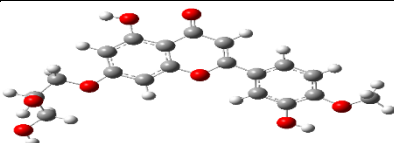
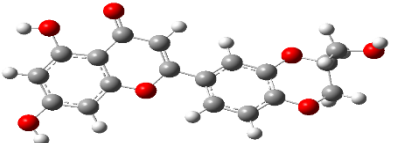
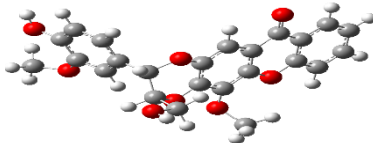
Table S1. PubChem chemical IDs, optimized structures and binding energies of 314 drug-like chemical compounds obtained from PubChem free database. 61 compounds with lower binding energies in comparison with DHM have been highlighted.

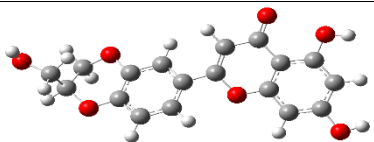
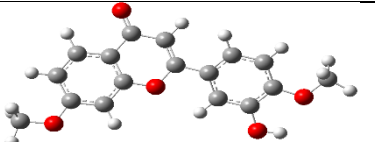
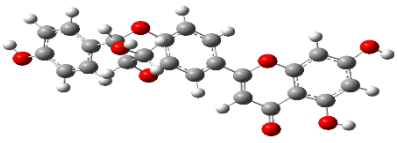
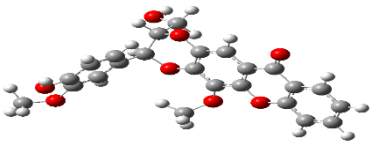
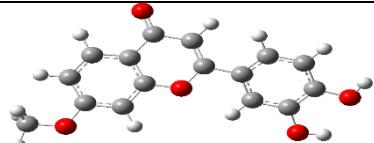
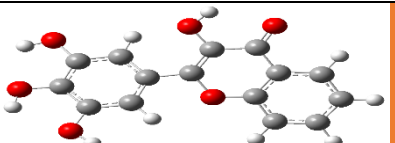
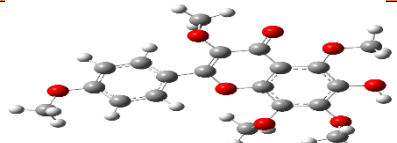
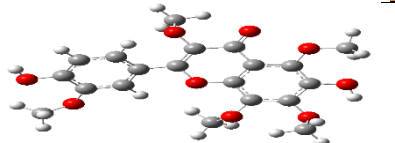
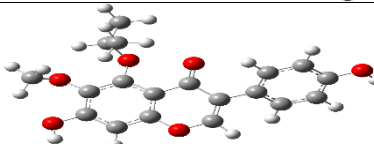
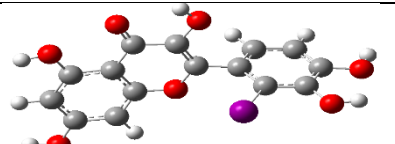
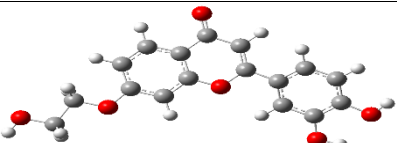
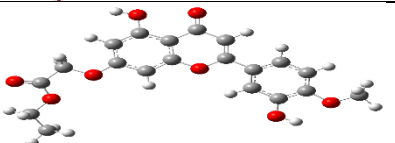
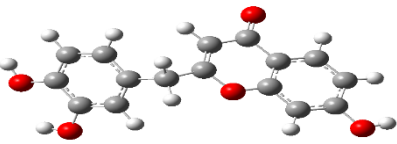
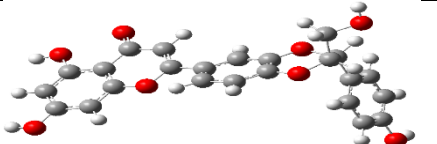
PubChem ID	Optimized structure	Binding Energy/kcal.mol ⁻¹	PubChem ID	Optimized structure	Binding Energy/kcal.mol ⁻¹
		TPSA/Å ²			TPSA/Å ²
1880		-4.8	26034		-5.3
		70.67			109.36
88281		-5.0	159026		-5.6
		90.89			74.23
190366		-6.2	245874		-4.6
		116.84			74.24
378687		-5.5	442410		-5.0
		68.91			86.99
580166		-6.3	639314		-6.0
		107.60			107.60
688853		-6.1	764011		-6.0
		90.89			96.22

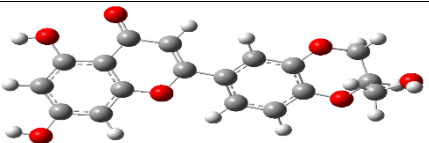
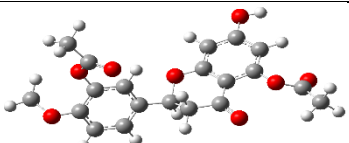
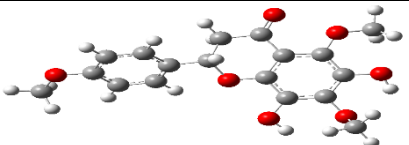
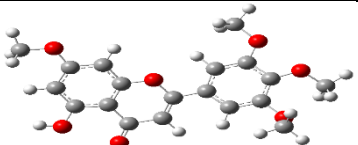
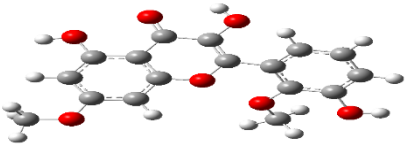
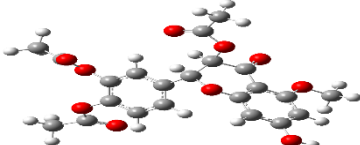
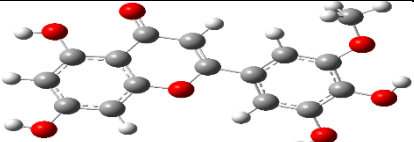
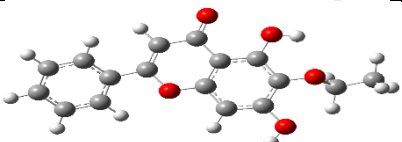
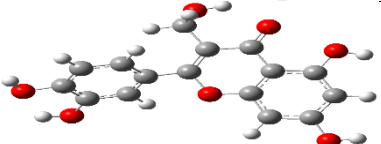
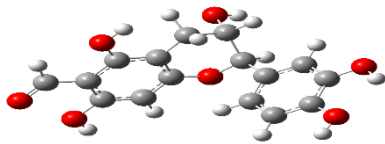
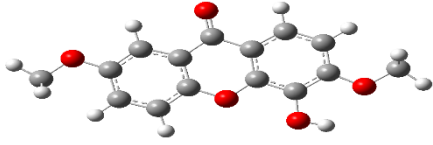
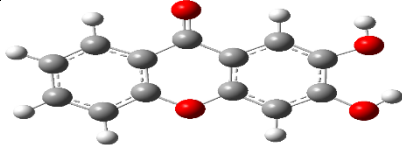
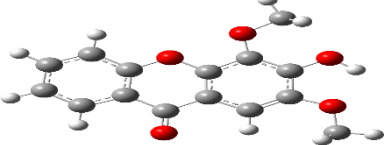
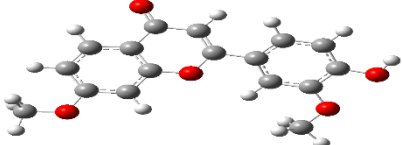
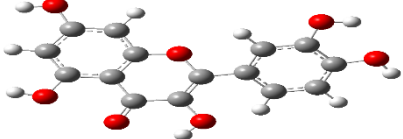
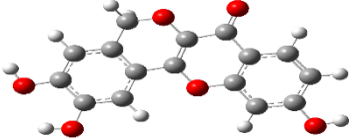
3512634		-5.3	5280343		-5.6
		86.99			131.35
5280445		-5.4	5280616		-5.9
		111.12			131.35
5280666		-5.2	5281604		-5.6
		100.13			120.36
5281605		-5.9	5281612		-5.4
		90.89			100.13
5281618		-5.1	5281638		-5.4
		79.90			131.35
5281642		-5.6	5281649		-4.9
		131.35			131.35
5281654		-5.4	5281665		-5.5
		120.36			111.12
5281676		-5.3	5281691		-5.7
		118.60			120.36

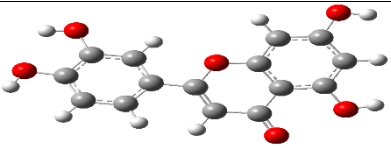
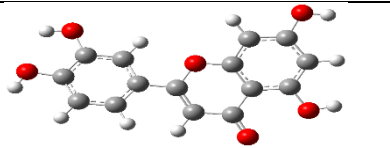
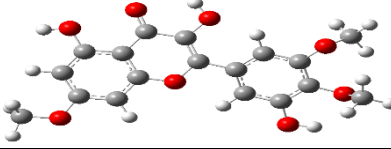
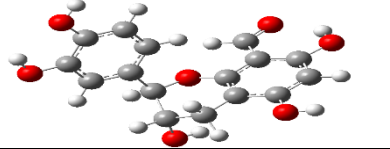
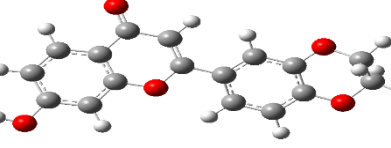
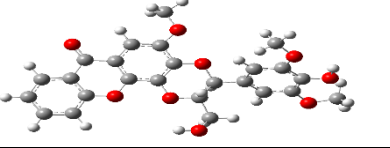
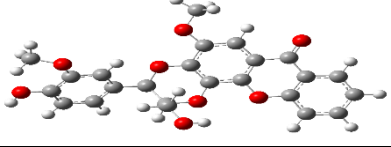
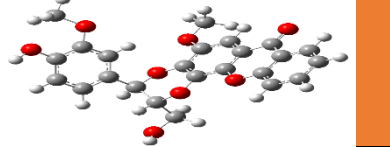
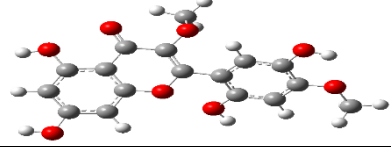
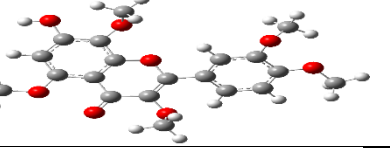
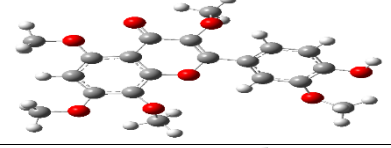
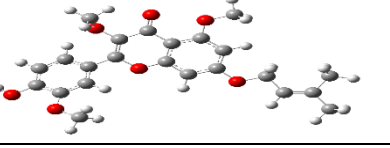
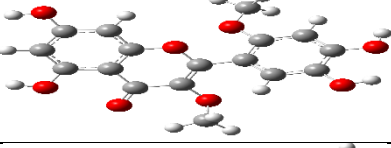
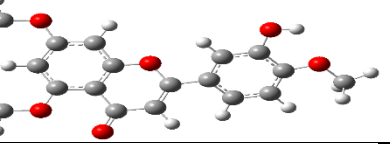
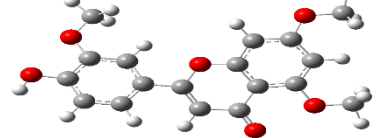
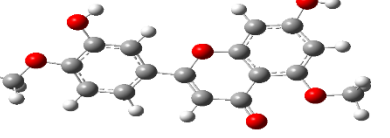
5281697		-5.6	5281699		-5.9
		111.12			120.36
5281701		-5.8	5281702		-5.1
		131.35			109.36
5281953		-5.0	5315125		-6.4
		129.59			111.12
5315126		-6.7	5315857		-4.4
		131.35			107.60
5318214		-5.6	5320287		-5.5
		100.13			109.36
5320428		-5.4	5320496		-4.8
		109.36			89.14
5320825		-5.5	5320945		-5.4
		127.83			109.36
5321864		-5.4	5322065		-5.5
		111.12			90.89

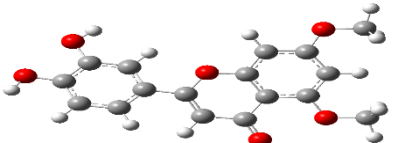

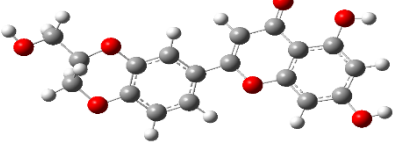
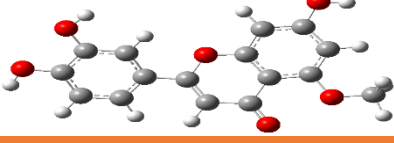
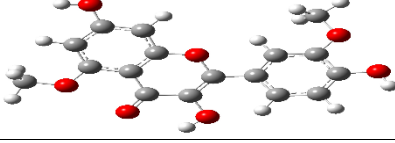
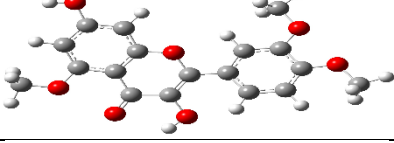
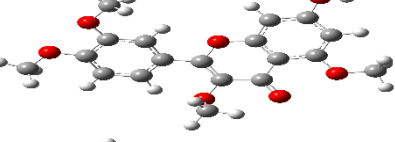
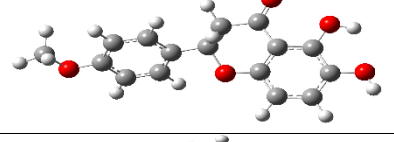
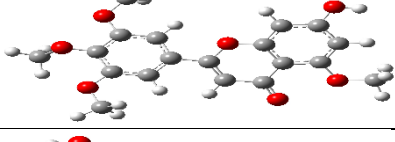
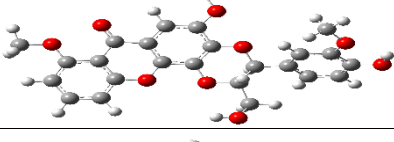
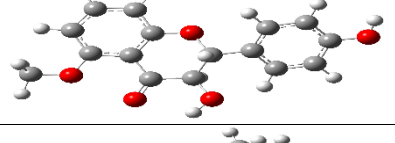
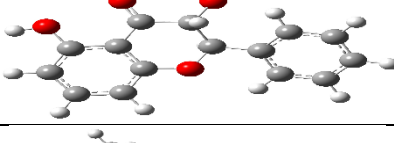
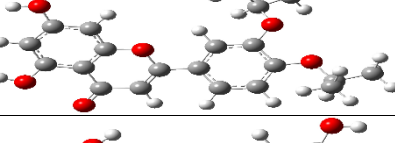
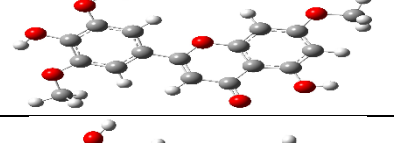
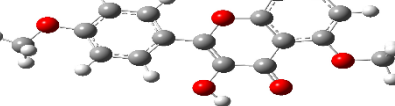
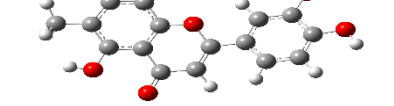
5323559		-4.2	5351234		-4.7
		118.60			89.14
5377945		-5.6	5378220		-5.5
		120.36			79.90
5379265		-5.1	5393164		-5.1
		98.37			111.12
5459196		-5.4	5464381		-4.9
		109.36			89.14
5467201		-6.7	5481236		-5.3
		118.60			100.13
5481248		-5.4	5487855		-5.0
		118.60			109.36
5488150		-5.3	5488643		-5.0
		89.14			109.36

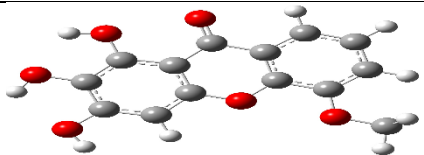
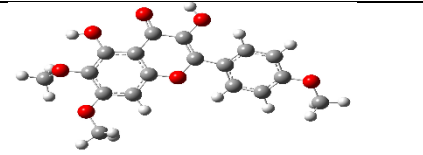


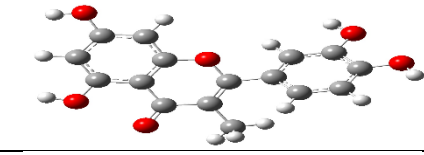
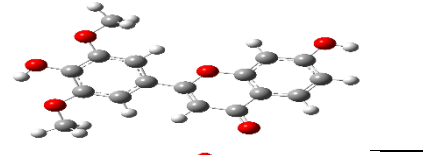
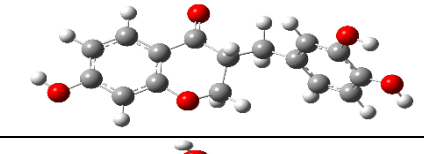
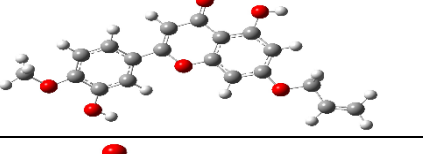
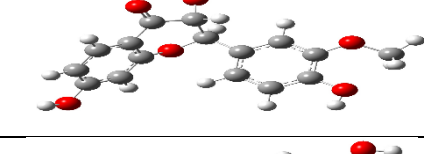
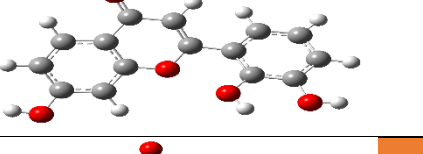
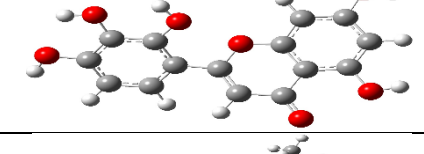
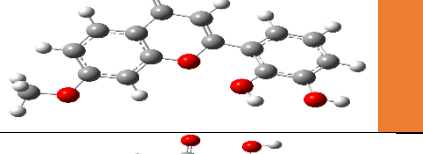
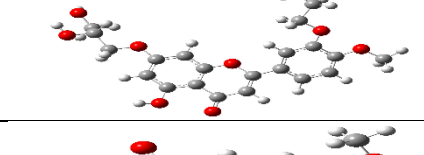
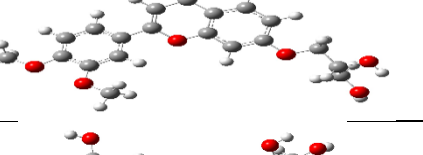
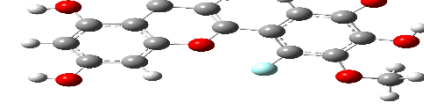
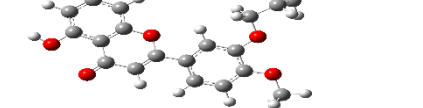
44258278		-5.3	5491448		-5.1
		120.36			118.60
5496473		-5.6	5496476		-5.2
		109.36			98.37
5704578		-5.4	5748558		-4.4
		109.36			98.37
6280229		-7.0	6452329		-5.7
		118.60			140.59
6477684		-6.0	6477685		-6.2
		90.89			111.12
7019535		-5.2	7330522		-5.0
		118.60			118.60
9888259		-4.6	9951473		-5.2
		138.82			129.59
10020234		-5.5	10320814		-5.6
		109.36			107.60

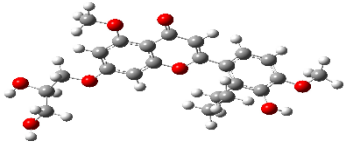
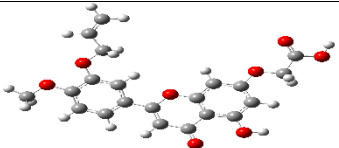
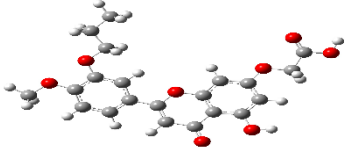
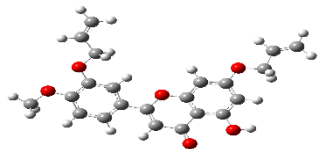
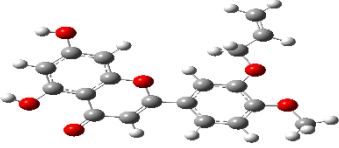
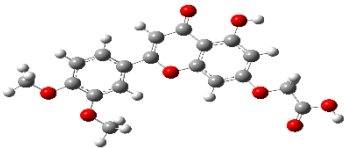
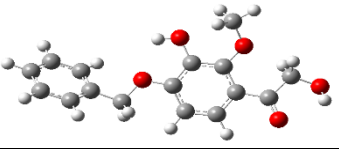
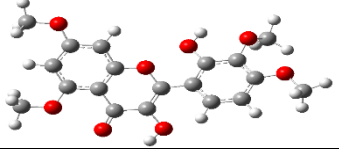
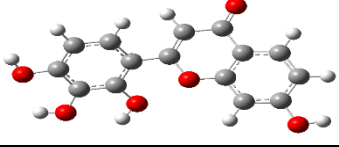
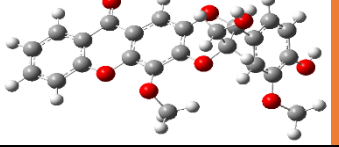
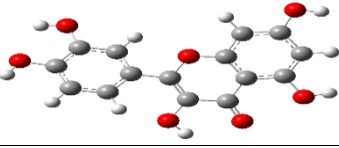
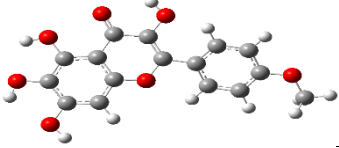
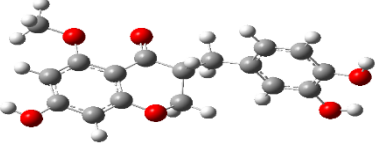
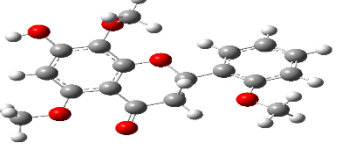
10337415		-4.8	10379917		-5.8
		109.36			68.91
10433042		-5.3	10455672		-5.6
		129.59			107.60
10493280		-6.0	10517292		-6.0
		79.90			111.12
10524310		-5.3	10525257		-5.2
		96.61			116.84
10545226		-4.7	10598612		-5.2
		89.14			131.35
10615139		-6.0	10620154		-5.0
		100.13			115.44
10636768		-5.1	10646467		-5.7
		90.89			129.59

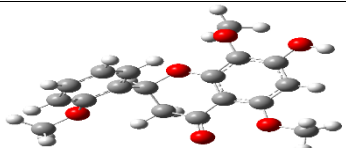
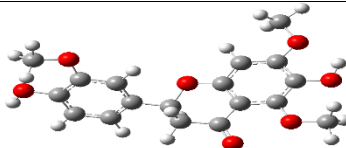
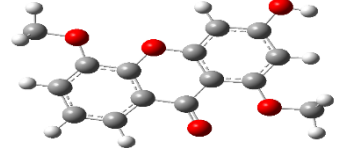
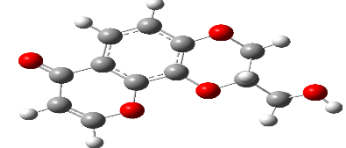
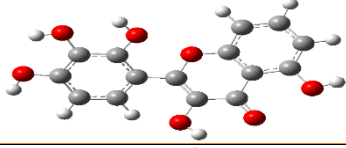
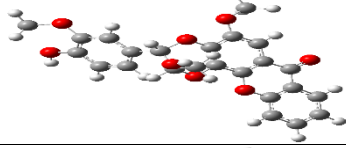
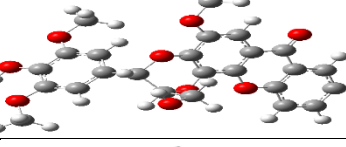
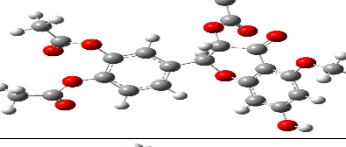
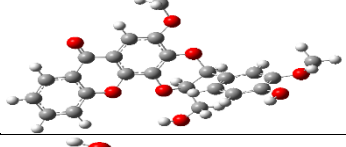
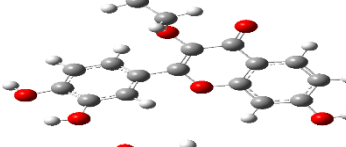
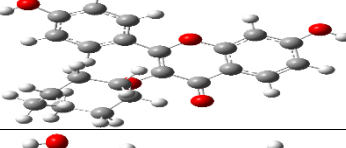
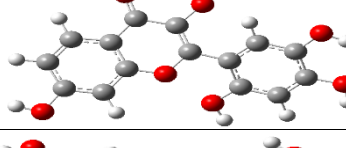
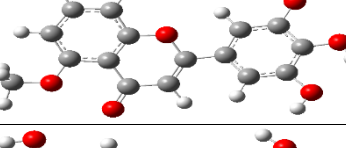
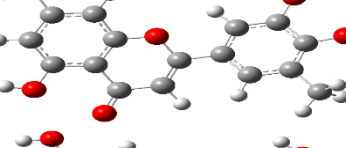
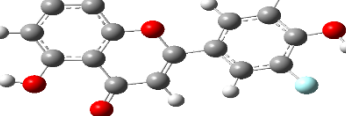
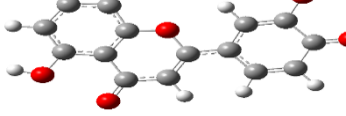
10807220		-5.1	10861984		-5.8
		109.36			108.38
10947972		-5.3	10970376		-5.2
		94.46			87.38
11012936		-4.7	11247770		-4.8
		109.36			134.68
11267045		-5.4	11300972		-5.4
		120.36			79.90
11347622		-5.6	12042311		-5.7
		131.35			127.44
12133313		-5.1	12214328		-5.7
		68.91			70.67
12214333		-5.2	12261165		-5.0
		68.91			68.91
12305312		-5.1	12314036		-5.7
		131.35			100.13

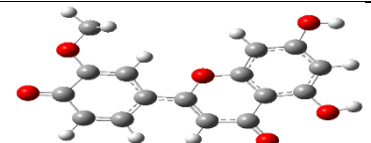
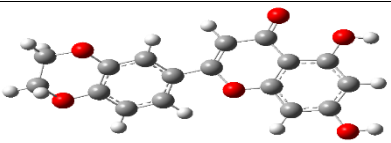
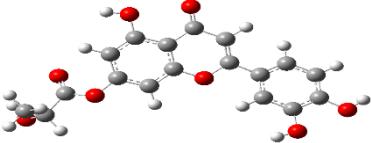
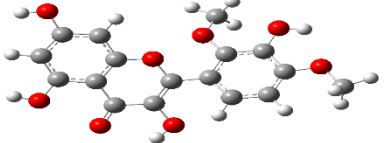
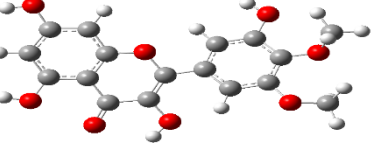
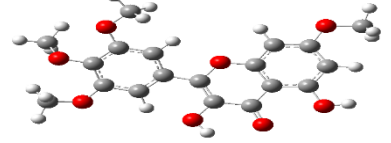
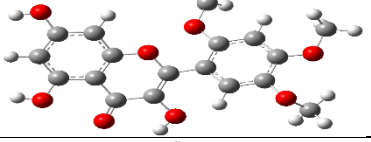
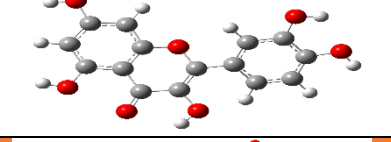
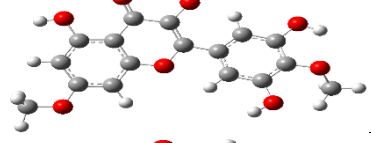
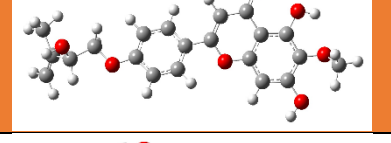
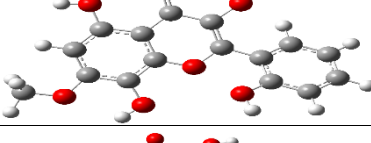
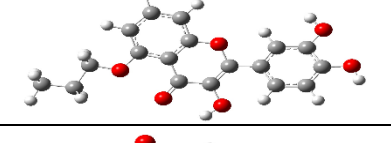
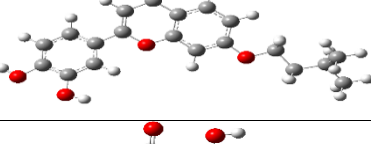
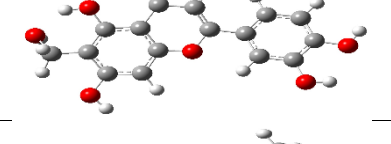
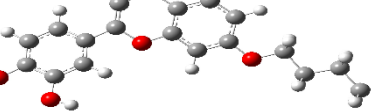
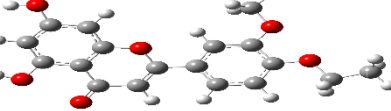
12359024		-5.9	12359025		-5.8
		111.12			111.12
12532439		-5.5	13259662		-5.0
		118.60			127.44
13349170		-6.3	13834089		-5.6
		68.91			116.84
13834127		-5.6	13834128		-6.3
		107.60			107.60
13915678		-5.3	13916267		-5.0
		129.59			96.61
13942544		-5.3	13942545		-5.5
		96.61			87.38
13942681		-5.0	13964545		-5.7
		129.59			78.14
13964546		-4.8	13964547		-5.8
		78.14			89.14

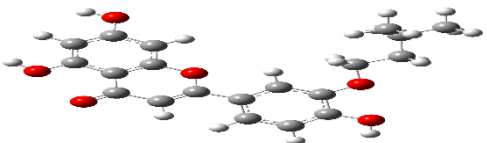
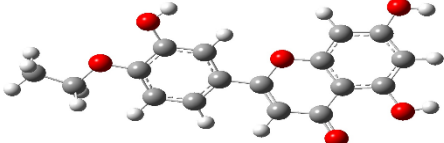
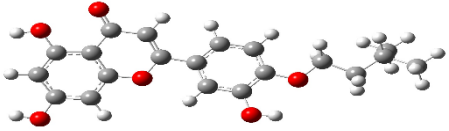
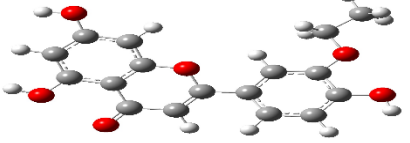
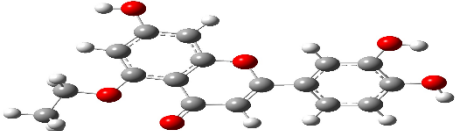
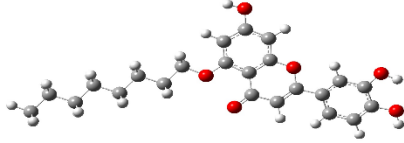
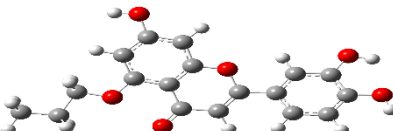
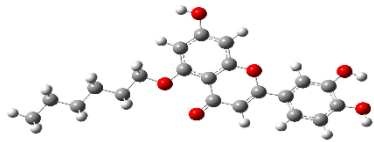
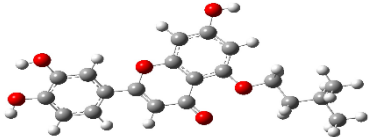
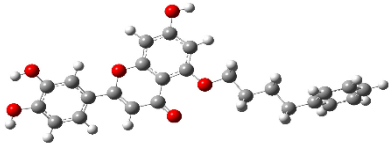
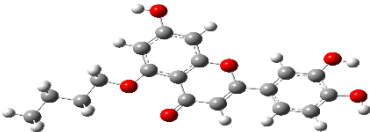
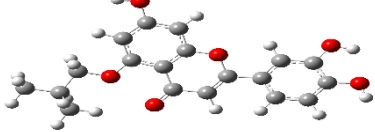

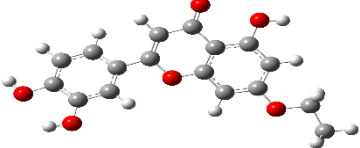
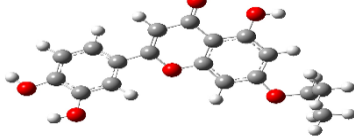
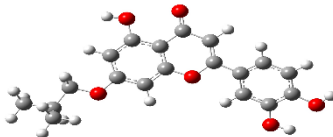
13964548			-5.8	13964549			-5.5
			89.14				89.14
10664985			-5.9	13964550			-5.9
			109.36				100.13
14162696			-5.6	14234929			-4.8
			109.36				98.37
14259793			-5.1	14353344			-5.7
			87.38				76.00
14354990			-5.4	14427460			-6.4
			87.38				116.84
14794882			-5.4	15054680			-5.5
			96.22				66.76
15108682			-5.1	15222911			-5.1
			89.14				98.37
15227607			-5.6	15293760			-5.8
			109.36				111.12

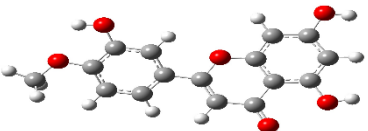
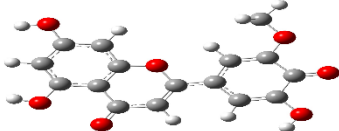
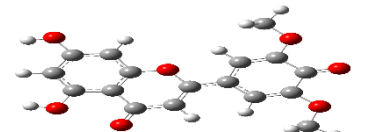
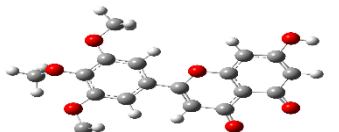
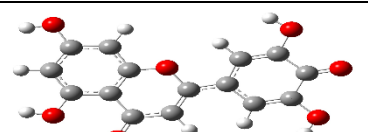
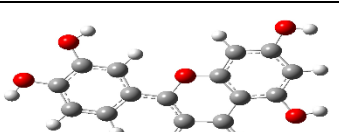
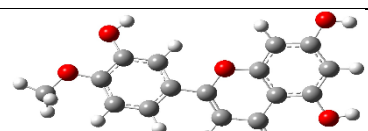
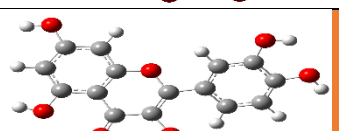
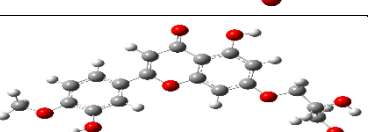
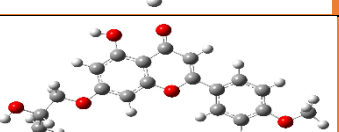
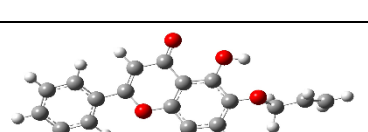
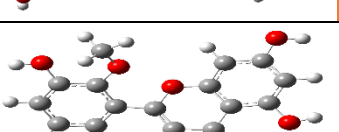
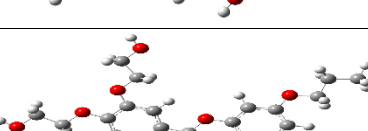
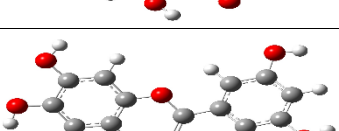
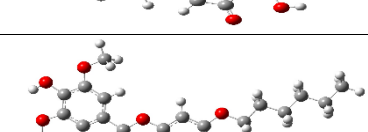
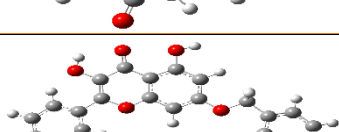
15379040		-5.6	15560536		-5.1
		100.13			98.37
15560612		-5.9	15614392		-5.2
		100.13			126.43
15661823		-5.4	15693661		-5.3
		111.12			89.14
15703606		-5.0	15814159		-5.2
		86.99			89.14
16093656		-5.0	16662883		-4.6
		96.22			90.89
9549306		-5.6	18542127		-6.3
		124.29			79.90
19049226		-5.2	19049238		-5.8
		118.60			118.60
18778787		-4.8	19049246		-5.3
		109.36			129.59

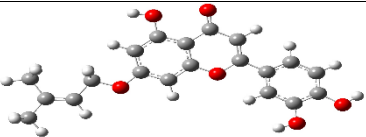
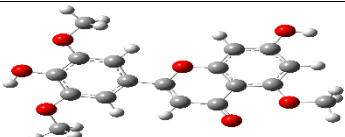
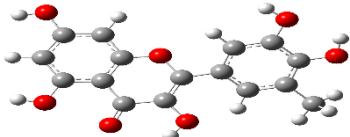
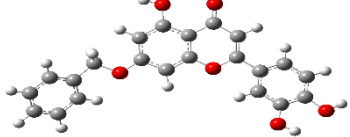
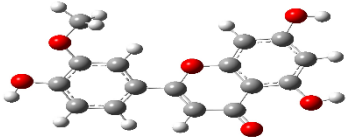
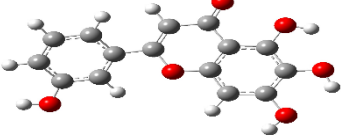
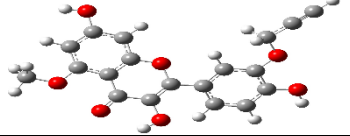
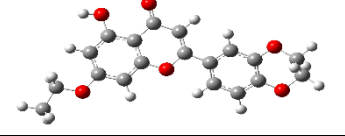
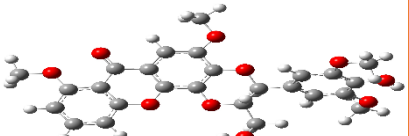
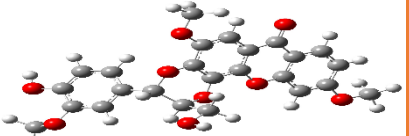
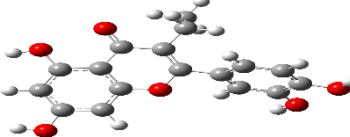
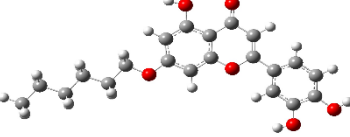
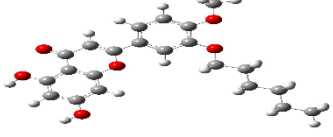
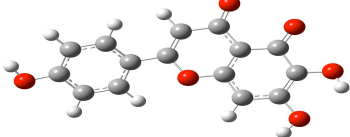
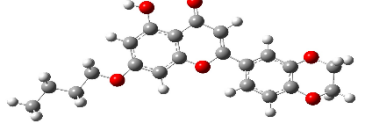
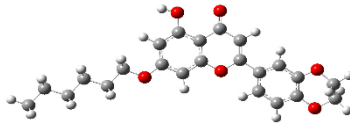
19049277		-5.1	19065204		-5.7
		118.60			115.44
19065213		-5.4	19065216		-5.0
		115.44			78.14
19065246		-4.9	19358582		-5.8
		89.14			115.44
19358620		-5.0	19890110		-5.2
		76.00			107.60
21158518		-5.8	21595562		-6.2
		111.12			107.60
21600688		-5.5	21633676		-5.2
		131.35			120.36
21676257		-5.0	21721829		-4.6
		96.22			74.23

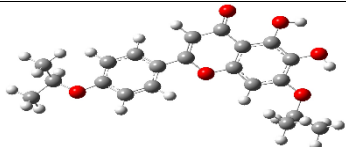
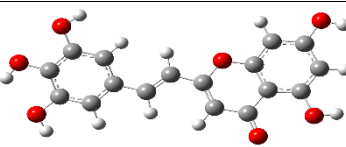
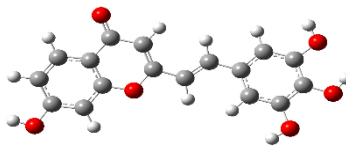
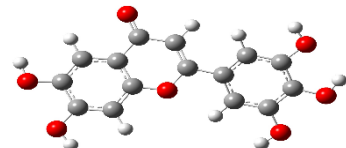

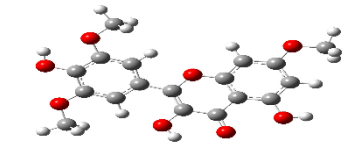
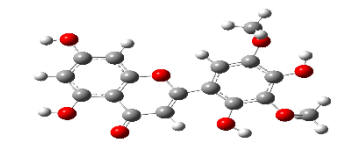
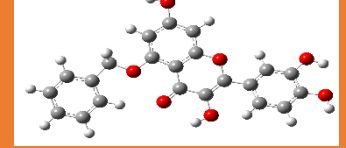
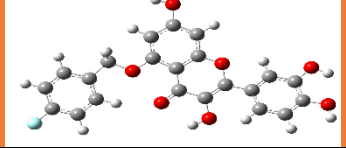
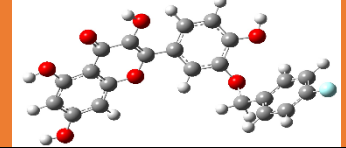
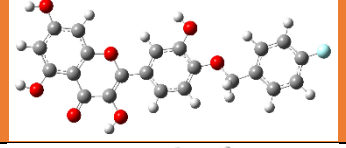
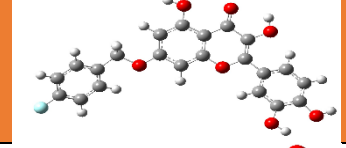
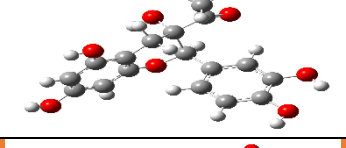
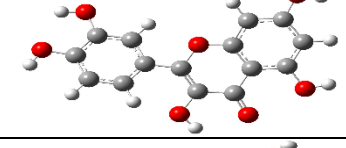
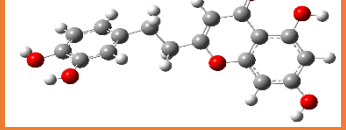
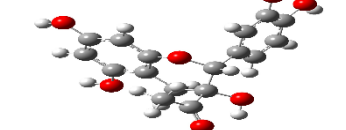
21636238			-5.1	21721836			-5.5
			74.23				94.46
21767017			-4.7	22324458			-4.6
			68.91				68.91
22339062			-6.0	23242592			-5.6
			131.35				107.60
23242593			-4.8	23247874			-4.9
			116.84				134.68
23259520			-5.5	23320229			-5.7
			107.60				100.13
23630406			-6.4	24721675			-5.8
			100.13				131.35
25030204			-5.7	25189537			-6.0
			120.36				111.12
25189611			-5.5	25201972			-5.7
			111.12				113.95

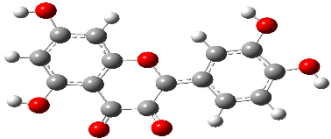
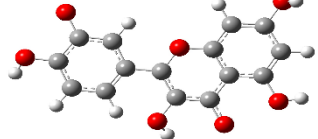
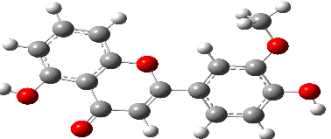
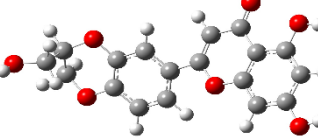
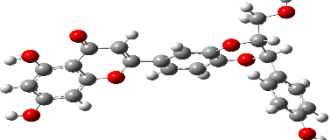
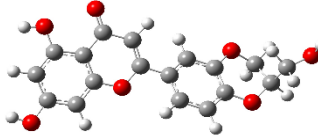
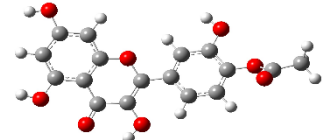
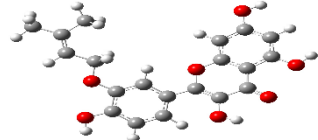
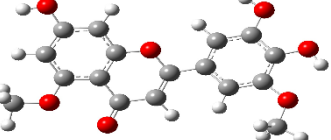
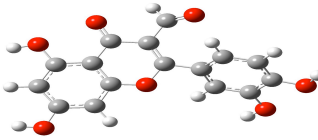
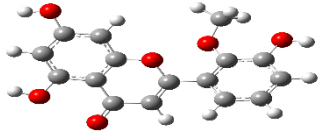
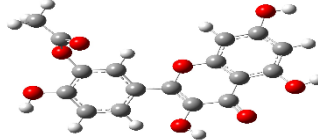
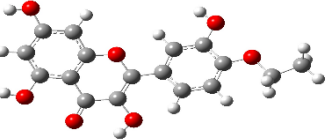
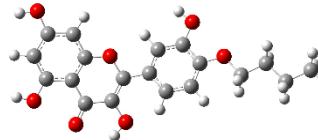
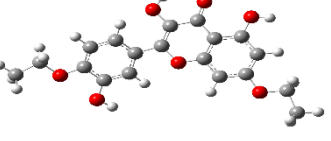
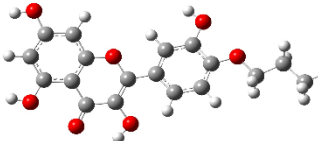
25203524		-5.6	25267158		-6.2
		102.96			89.14
44258150		-6.1	44259518		-5.4
		137.43			129.59
44259511		-5.5	44259639		-5.5
		129.59			107.60
44259523		-5.0	5280343		-5.6
		118.60			131.35
44259638		-5.7	57381727		-5.9
		129.59			109.36
44259903		-6.1	57402278		-5.5
		120.36			120.36
44608108		-5.5	58076345		-5.6
		100.13			131.35
44608109		-5.5	44608113		-5.2
		100.13			89.14

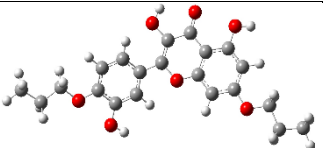
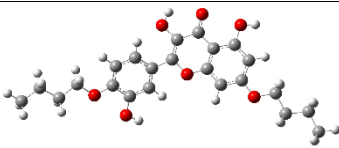
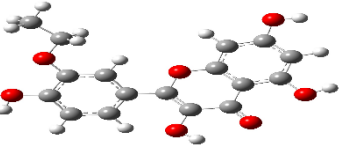
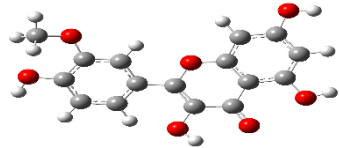
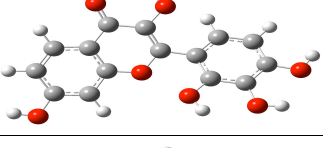
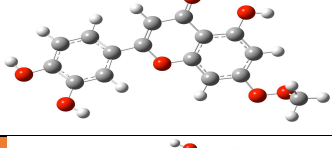
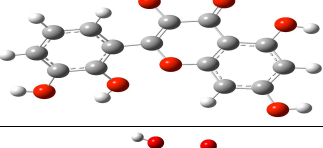
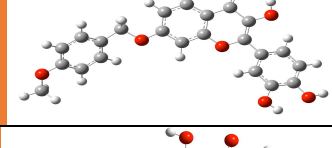
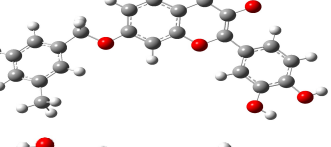
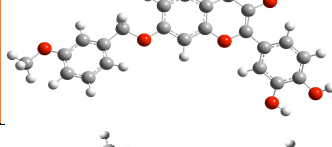
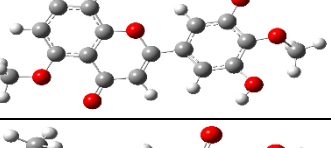
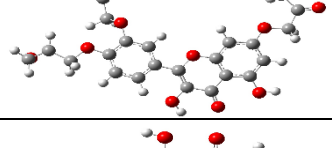
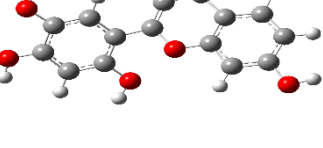
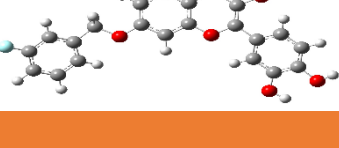
44608260		-4.6	44608261		-5.7
		100.13			100.13
44608262		-5.3	44608263		-5.1
		100.13			100.13
44610309		-5.3	44610310		-5.5
		100.13			100.13
44610311		-5.5	44610313		-5.1
		100.13			100.13
44610314		-5.8	44610473		-6.1
		100.13			100.13
44610474		-5.2	44610475		-5.6
		100.13			100.13
44610476		-5.7	44610477		-4.8
		100.13			100.13
44610478		-5.9	44610479		-5.0
		100.13			100.13

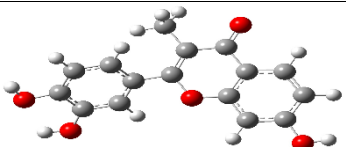
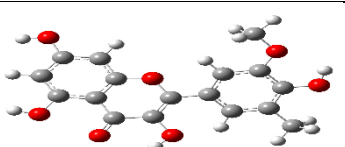
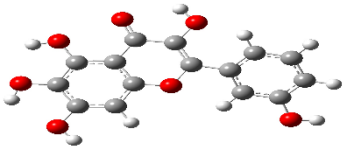
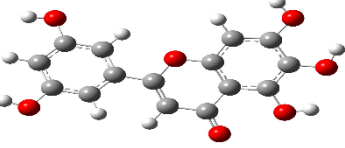
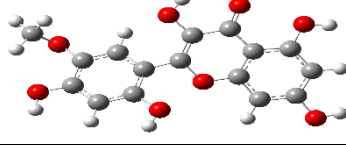
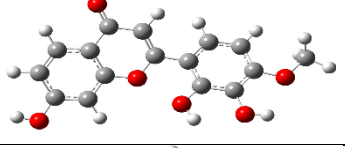
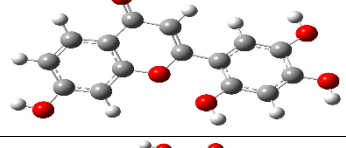
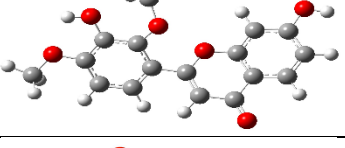
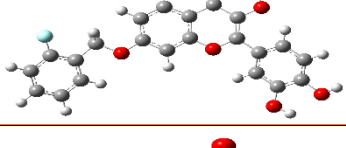
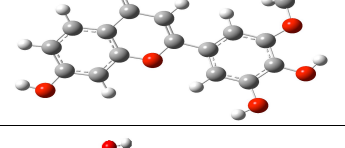
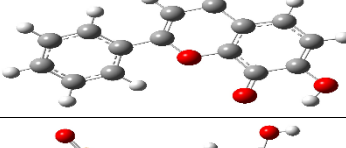
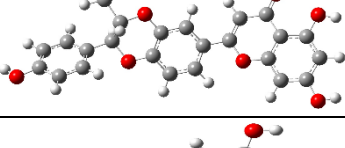
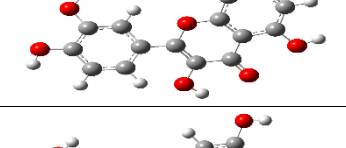
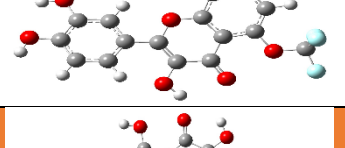
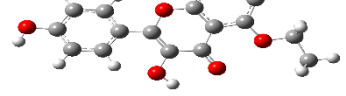
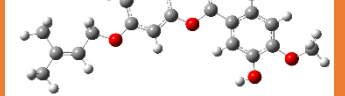
46781386		-5.1	46878515		-5.4
		100.13			123.19
46878516		-4.9	46878517		-4.9
		112.19			101.20
46878558		-5.8	46906036		-5.2
		134.18			134.18
49849634		-5.4	49849859		-6.0
		100.13			131.35
53819694		-5.7	53819695		-5.9
		129.59			129.59
54760989		-5.0	56929794		-5.3
		79.90			120.36
59918405		-4.7	59991307		-5.9
		118.60			111.12
66684101		-5.1	67984060		-6.5
		98.37			120.36

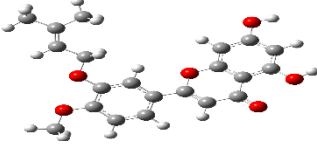
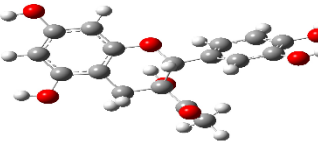
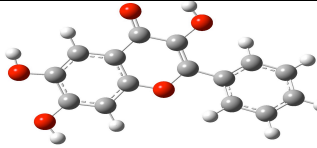
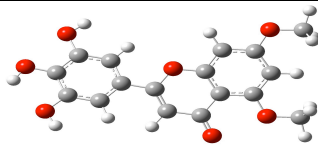
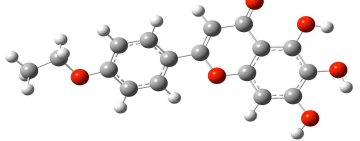
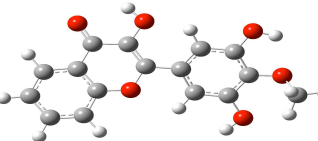
69211947		-5.8	69325736		-5.1
		100.13			98.37
70231225		-5.7	71313853		-6.7
		131.35			100.13
71314865		-5.5	71414490		-5.7
		100.13			111.12
71600119		-4.7	71723454		-5.7
		109.36			78.14
14427462		-6.5	14757915		-5.9
		126.07			116.84
70020252		-5.6	71723737		-5.4
		111.12			100.13
73897342		-5.0	86289526		-5.5
		89.14			113.95
71723456		-5.6	71723458		-5.2
		78.14			78.14

76311605		-5.8	76327075		-6.1
		89.14			131.35
76330740		-5.5	85981660		-5.8
		111.12			131.35
88462991		-5.8	90657702		-5.4
		131.35			118.60
88494854		-5.3	89781809		-6.2
		129.59			120.36
90643985		-6.5	90643986		-6.5
		120.36			120.36
90643987		-6.5	90643991		-6.7
		120.36			120.36
91028282		-5.5	91069955		-5.8
		127.44			131.35
91162275		-6.0	91228926		-5.5
		111.12			127.44

100985949		-6.1	100985950		-5.7
		128.18			128.18
100995351		-5.4	101064810		-6.1
		79.90			109.36
100968625		-7.1	101064811		-6.0
		129.59			109.36
101566521		-5.7	101675226		-5.9
		137.43			120.36
101914779		-5.7	129646445		-5.7
		109.36			128.19
102276010		-5.2	102292606		-5.7
		100.13			137.43
118711942		-5.8	118711944		-4.7
		120.36			120.36
118712001		-5.5	118711943		-5.6
		109.36			120.36

118712002		-5.5	118712003		-5.4
		109.36			109.36
123649972		-5.5	124202864		-5.6
		120.36			120.36
129648032		-5.8	129711975		-5.8
		131.35			109.36
129713895		-5.7	129825762		-6.0
		131.35			129.59
129825792		-6.9	129825797		-6.5
		120.36			129.59
129852329		-5.7	129868619		-5.2
		109.36			135.95
129882434		-5.4	129904975		-6.5
		120.36			120.36

130335262			-5.1	130335485			-4.9
			90.89				120.36
131831747			-5.6	131834556			-4.8
			131.35				120.36
131836638			-5.7	131837240			-5.8
			140.59				100.13
131837242			-5.3	131837258			-4.7
			111.12				89.14
129905005			-6.8	131839469			-5.6
			120.36				100.13
134820127			-5.4	134836277			-5.9
			73.50				129.59
137010076			-5.6	138112436			-4.6
			137.43				120.36
138112463			-5.9	139080697			-5.9
			120.36				109.36

139593046		-4.8	140279985		-5.7
		89.14			127.44
141151974		-5.7	141256537		-5.5
		90.89			109.36
141312957		-5.2	141806715		-5.8
		100.13			100.13